Magnetic Fields of Massive Cores of DR21 Filament:

Virial Expanding Cores in a Virial Contracting Filament?

Tao-Chung Ching[1,2]

Shih-Ping Lai[1], Qizhou Zhang[2], Josep M. Girart[3,2], Keping Qiu[4], and Hauyu B. Liu[5]

[1]Institute of Astronomy, National Tsing-Hua University, Taiwan
[2]Harvard-Smithsonian Center for Astrophysics
[3]Institut de Ci`encies de l'Espai, (CSIC-IEEC), Spain
[4]Nanjing University, China
[5]European Southern Observatory, Germany

- Outline
  - DR21 filament and massive cores
    - Virial parameters of turbulent, magnetic, and gravitational energy
    - How to measure magnetic field (B-field) strength
    - DR21 filament and its massive cores
    - SMA data
    - Analysis & Conclusion
  - SMA polarization mosaic project

Introduction

- Molecular clouds: highly turbulent, magnetized, filamentary structures

CO J=1-0 emission

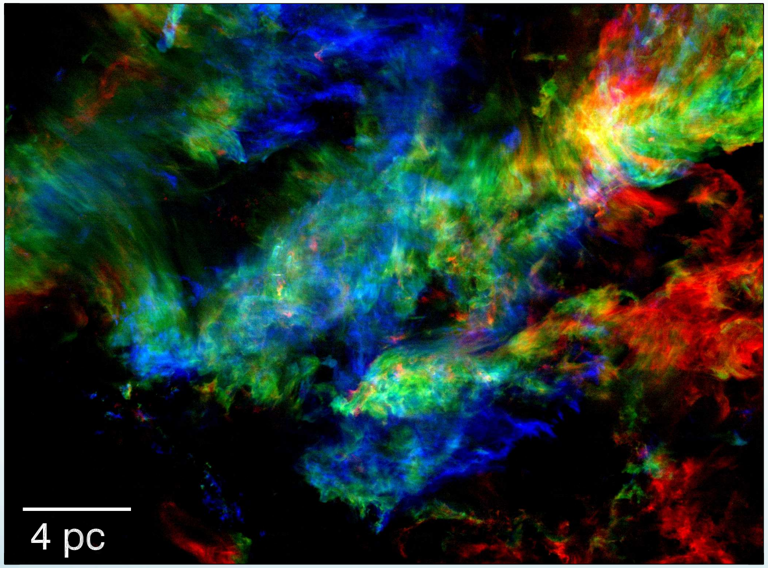

Narayanan et al. 2008

Extinction map and optical polarization

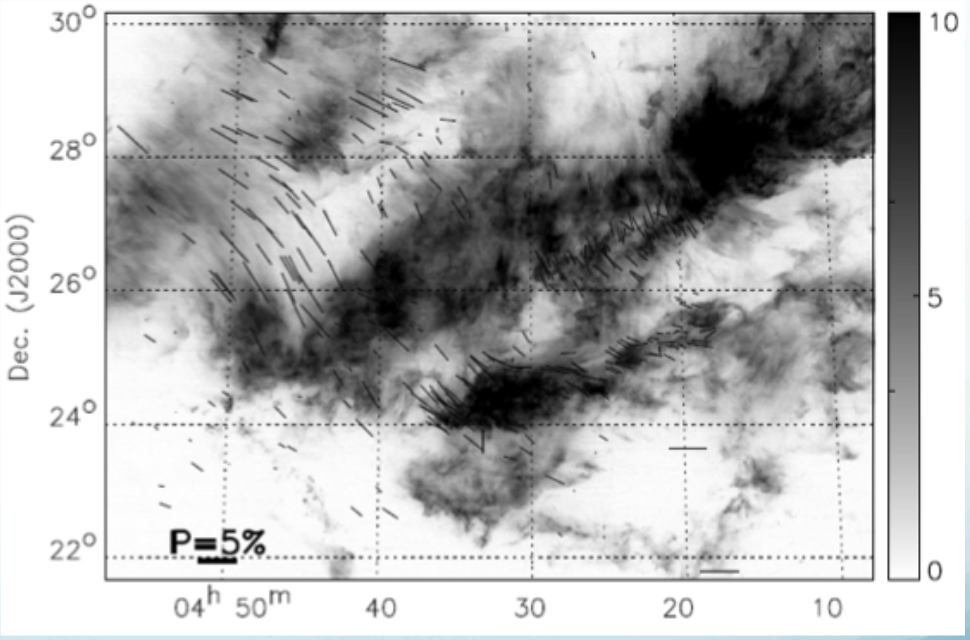

Goldsmith et al. 2008

- Virial theorem

$$\frac{1}{2}\ddot{I} = 2(\mathcal{T} - \mathcal{T}_0) + \mathcal{M} + \mathcal{W}.$$

turbulence surface magnetic field self-gravity

  - *W*: negative, gravitational collapse
  - *T* & *M*: positive, support cloud against gravitational collapse
  - *I*: proportional to the inertia of the cloud
    - $(\ddot{I} > 0)$ expansion
    - $(\ddot{I} < 0)$ collapse

Self-gravity

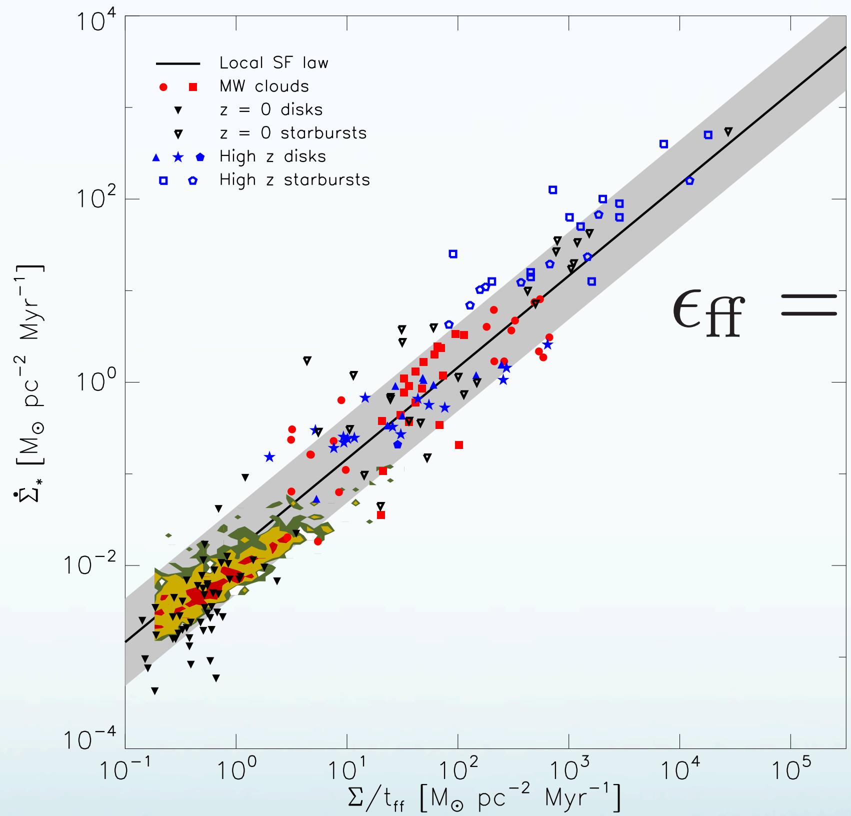

Column Density

SFR rate

$$\epsilon_{\rm ff} = 0.01$$

Krumholz et al. 2012

Turbulence

- Larson's Laws

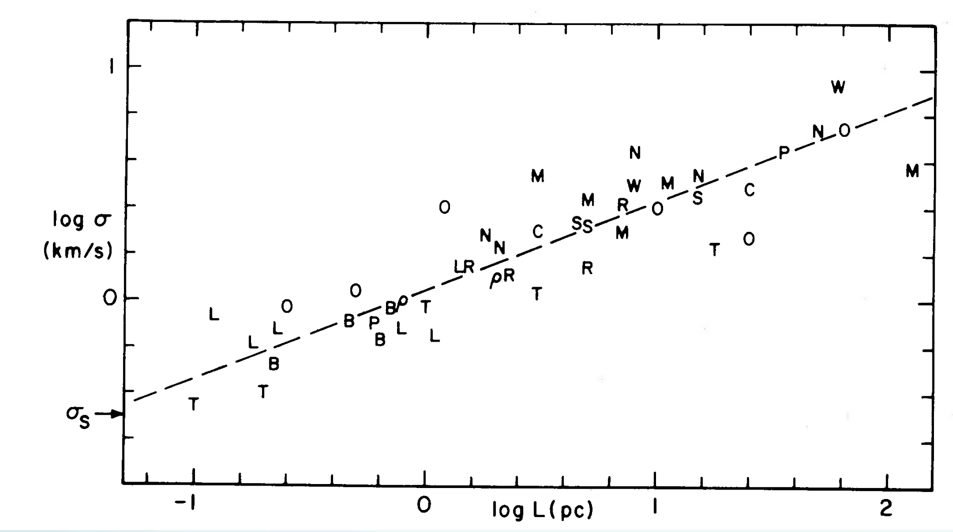

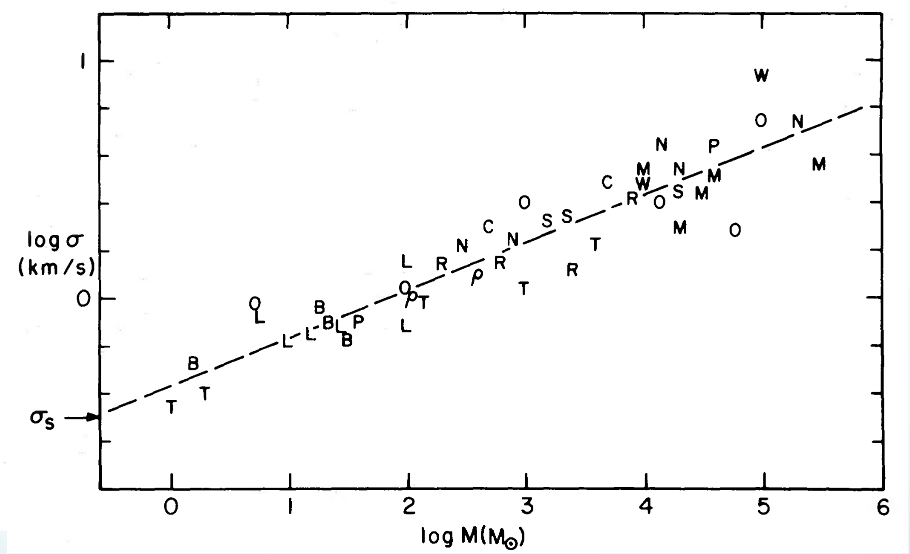

$$\sigma \propto L^{0.38}$$

$$\sigma\,(\mathrm{km\,s^{-1}}) = 0.42\,M(M_\odot)^{0.20}$$

- Log-normal probability distribution function

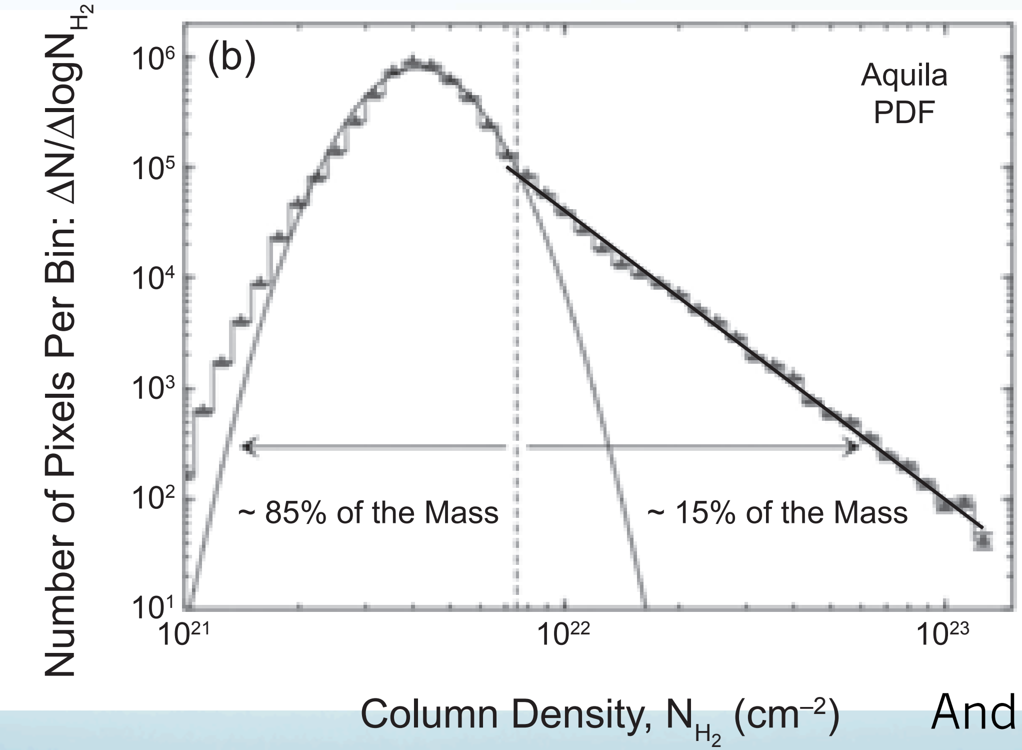

Andre et al. 2001

- reproduce of the filamentary structures of clouds

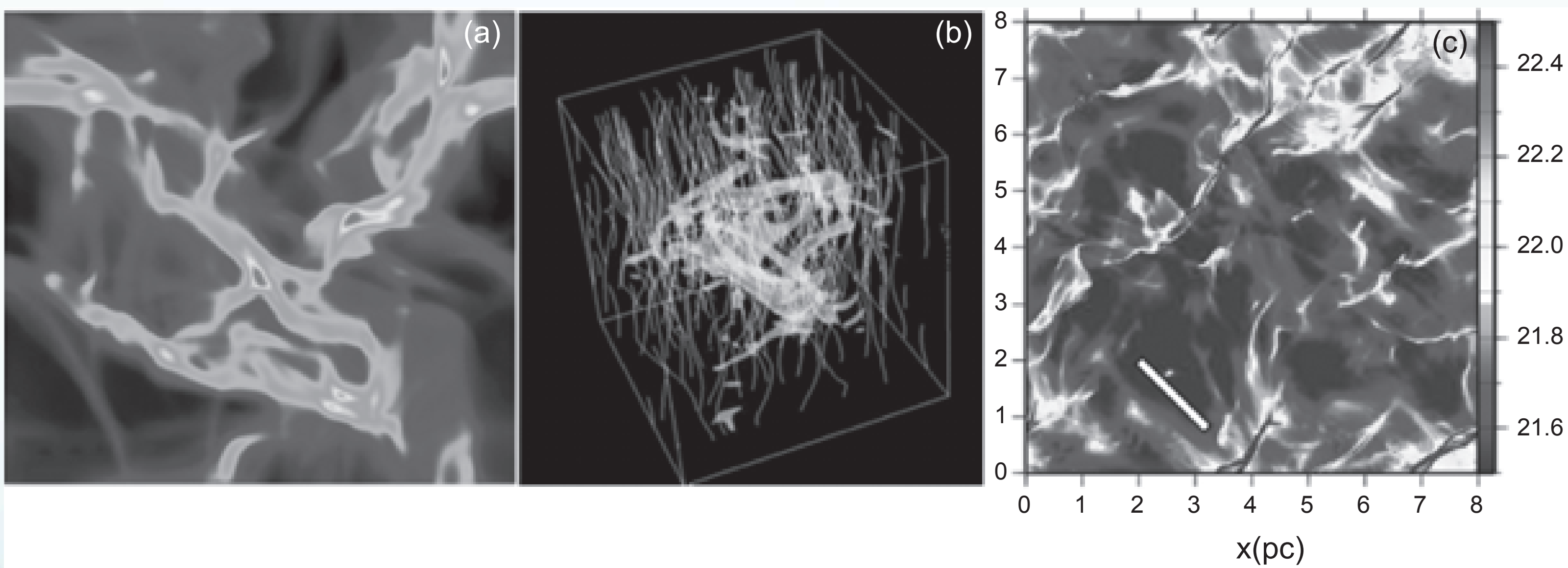

Padoan et al. 2001

Magnetic Field

$B^2 \sim M \sim n_H r^3$

$r \sim n_H^{1/3}$

- $B \sim n_H^k$
  - k = 2/3 for weak magnetic field models (flux conservation)
  - k = 0.4-0.5 for strong magnetic field models (ambipolar diffusion)

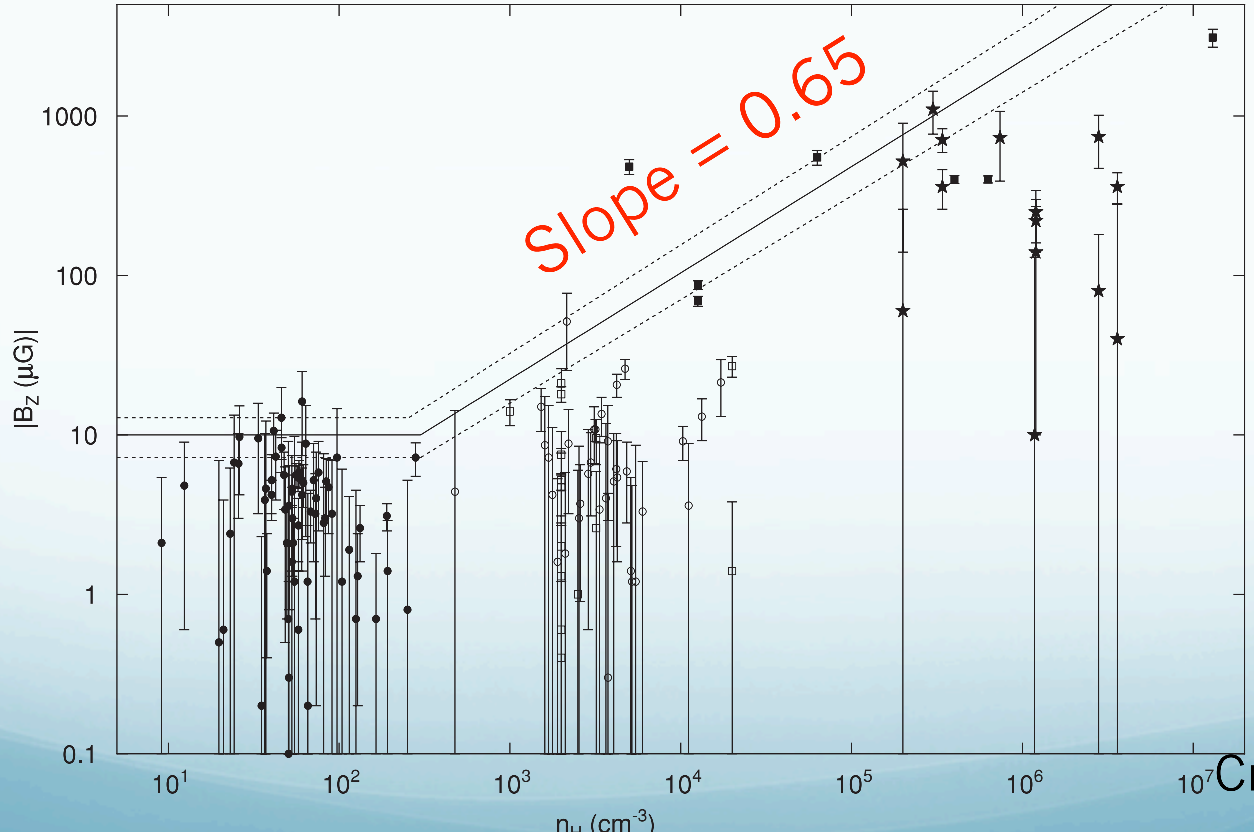

Crutcher et al. 2010

- Cloud Elongation v.s. Magnetic Field Orientation

Taurus Cloud

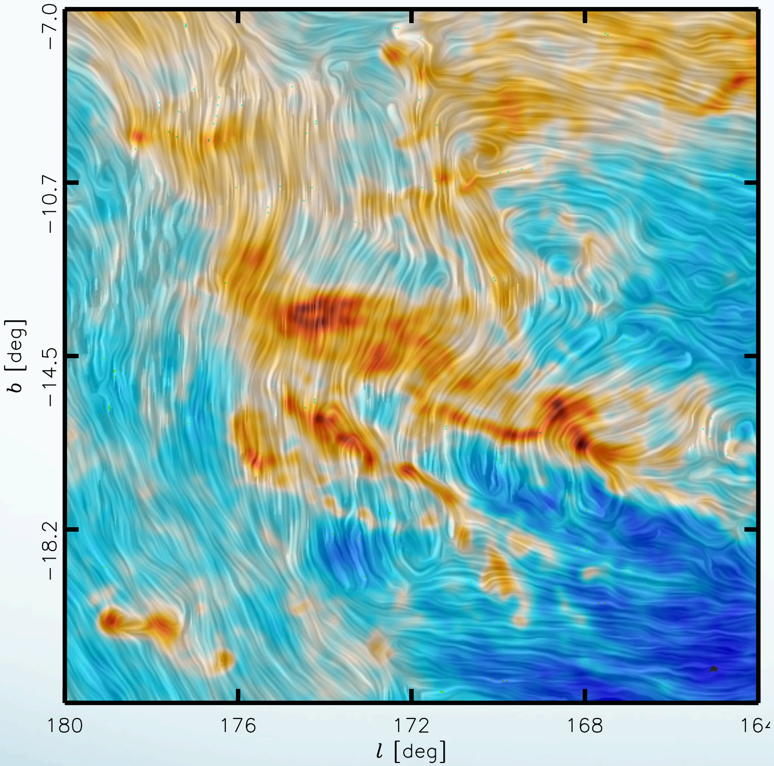

Planck XXXV 2015

L1495

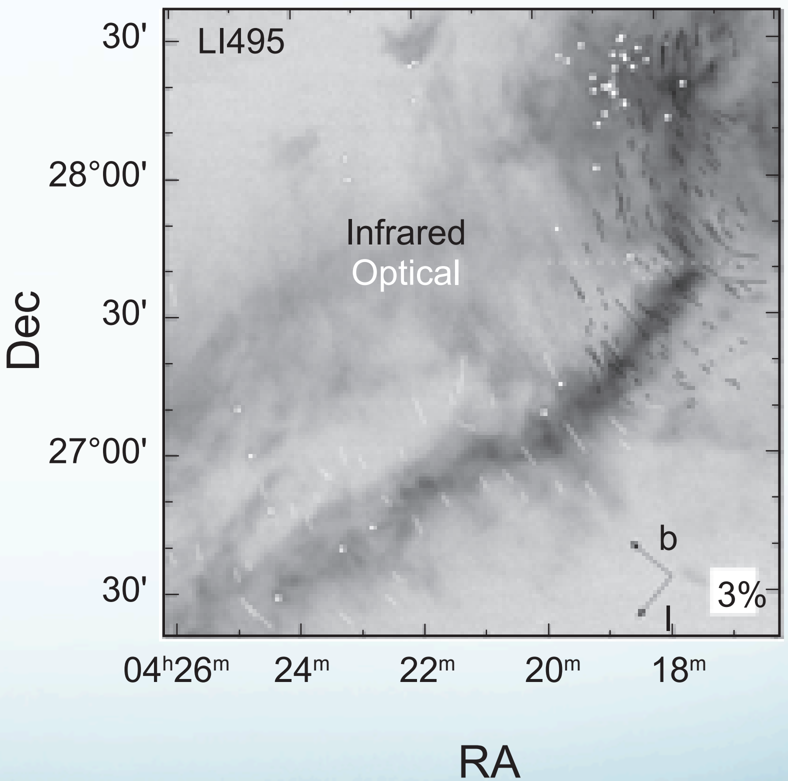

Chapman et al. 2011

- From 10 pc to 0.1 pc scales, molecular clouds appear to be either parallel or perpendicular to magnetic fields

10 pc Clouds

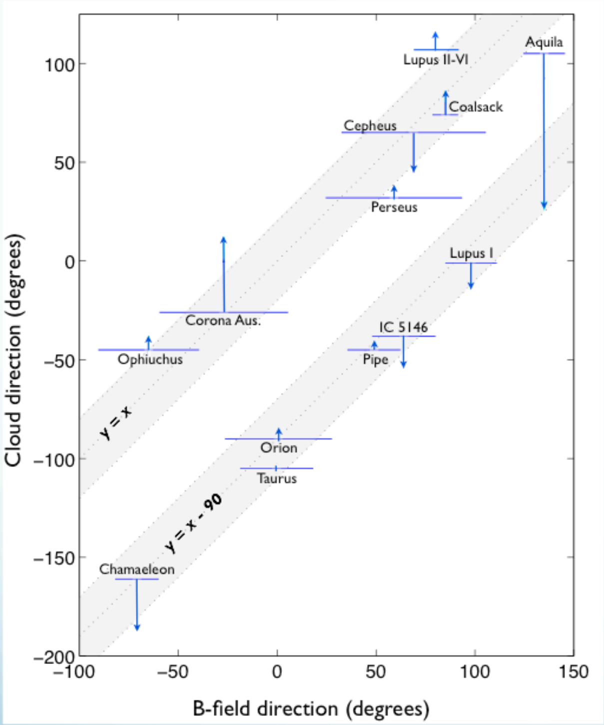

Li et al. 2013

1 pc Filaments

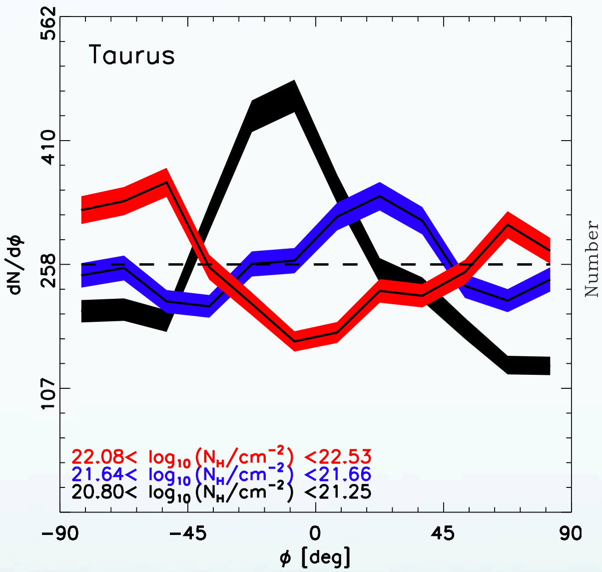

Planck XXXV 2015

0.1 pc Massive Cores

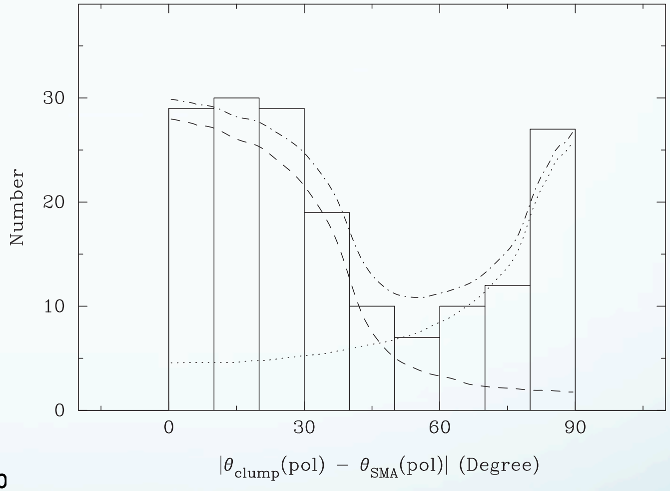

Zhang et al. 2014

- Magnetic field v.s. Turbulence

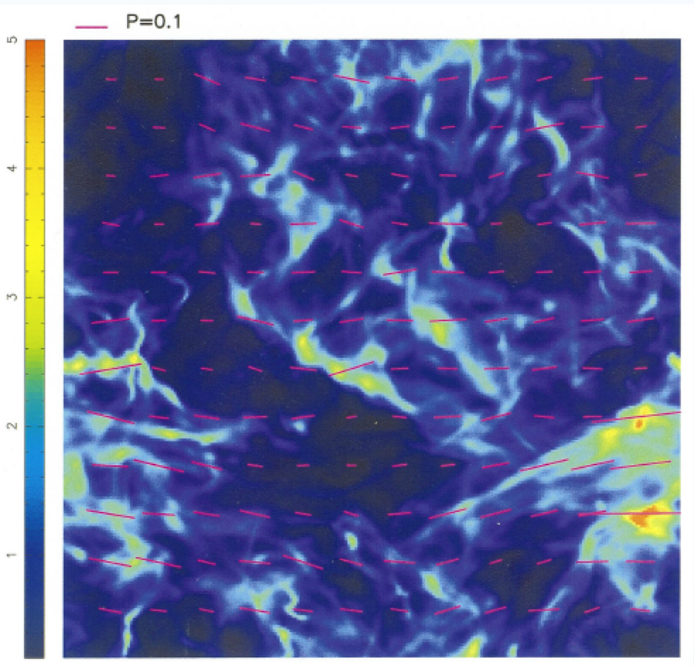

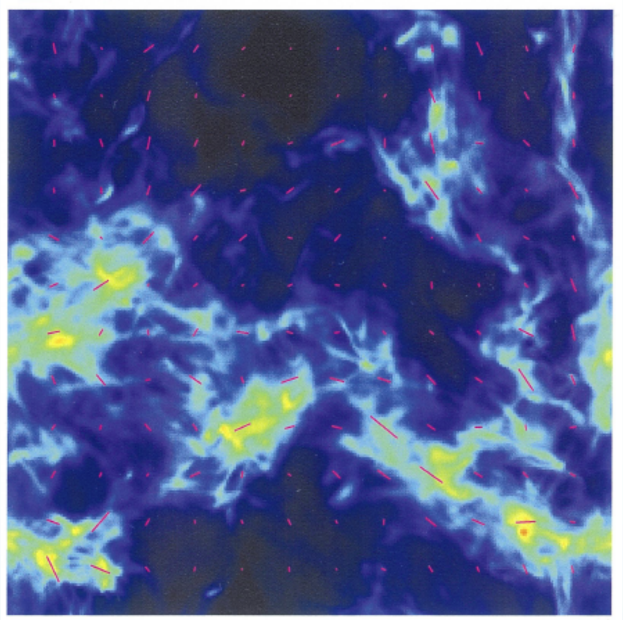

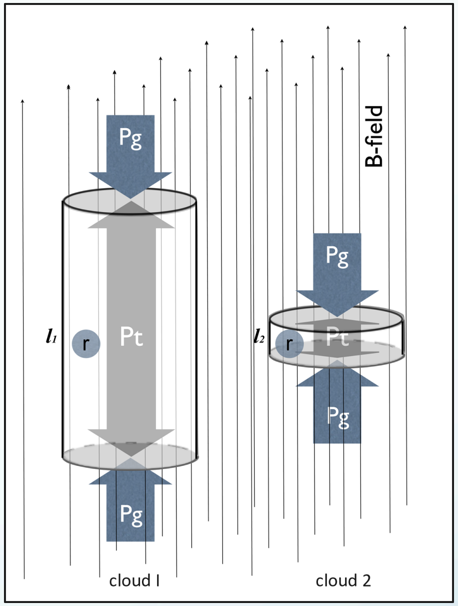

Ostriker et al. 2001

- Measure magnetic fields in molecular clouds
  - Zeeman effect
    - Measure magnetic field along the light of sight (B_{los})
    - The only way to directly measure magnetic field strength
  - Linearly polarized dust emission
    - Measure magnetic field on the plane of sky (B_{pos})
    - The Chandrasekhar–Fermi equation (CF equation; Chandrasekhar & Fermi 1953) gives estimation of magnetic field strength
  - Polarized molecular line emission (Goldreich-Kylafis effect)
    - The polarization direction could be either parallel or perpendicular to the magnetic field direction
  - Velocity dispersion measurements of molecular line emission
    - The ion molecular line width of ion is expected to be wider than the width of neutral

Polarization form Magnetically Aligned Dust Grains

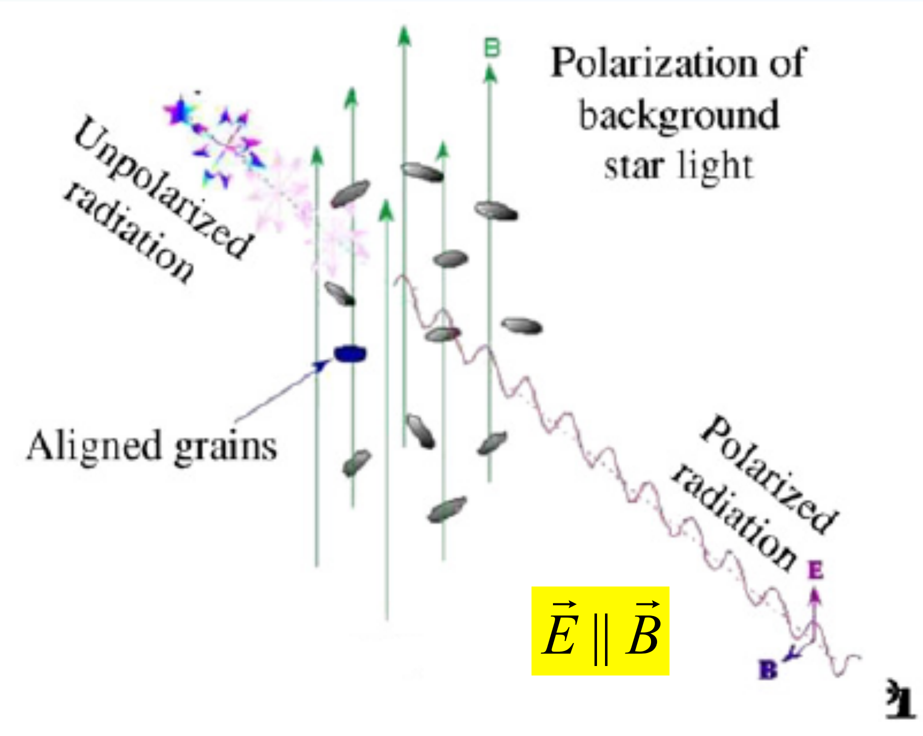

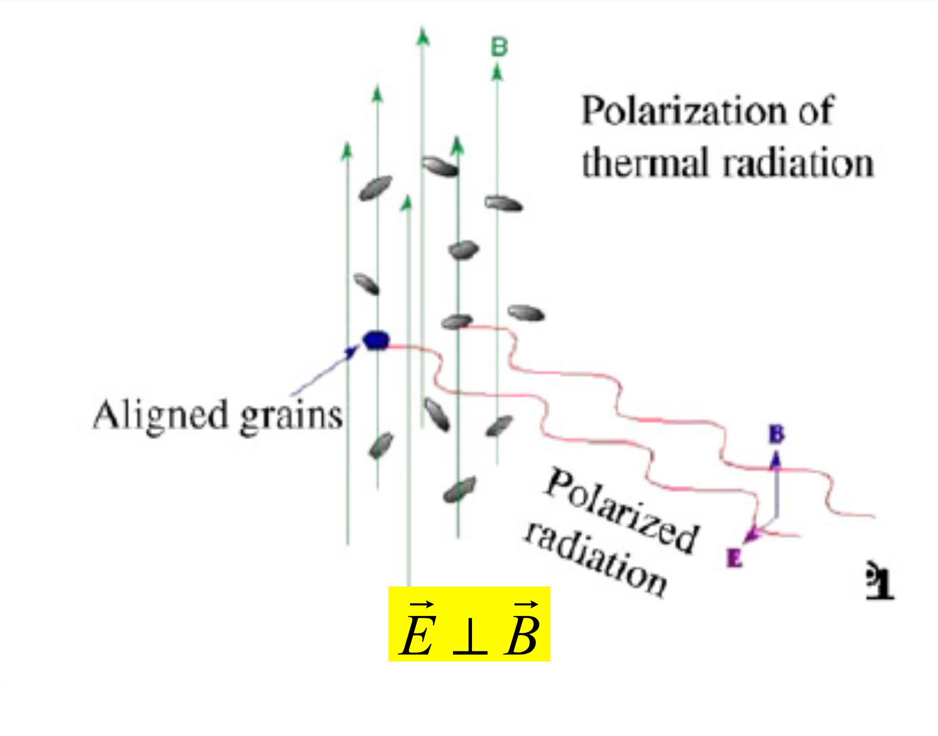

Optical, Near-Infrared
Selective Absorption

Far-Infrared, Submillimeter
Thermal Emission

- CF equation
  - 1953

$$\frac{\delta B}{B} \simeq \frac{\delta V_{los}}{V_A},$$

$$V_A = B/\sqrt{4\pi\rho} \text{ is the Alfvén speed}$$

  - Assume magnetic field model

$$\boldsymbol{B_p = Q\sqrt{4\pi\bar{\rho}}\,\frac{\delta v_{\mathrm{los}}}{\delta\phi}}\,,$$

  - Angular dispersion function (Hildebrand et al. 2009 ; Houde et al. 2009, 2011, 2016)

$$1 - \langle \cos\left[\Delta\Phi\left(l\right)\right]\rangle \simeq \sum_{j=1}^{\infty} a'_{2j} l^{2j} + \left[\frac{N}{1 + N\langle B_0^2\rangle/\langle B_t^2\rangle}\right]$$
$$\times \left\{\frac{1}{N_1}\left[1 - e^{-l^2/2(\delta^2+2W_1^2)}\right] + \frac{1}{N_2}\left[1 - e^{-l^2/2(\delta^2+2W_2^2)}\right] - \frac{2}{N_{12}}\left[1 - e^{-l^2/2(\delta^2+W_1^2+W_2^2)}\right]\right\},$$

$$\langle B_0^2\rangle^{1/2} = \sqrt{4\pi\rho}\,\delta V_{los}\left[\frac{\langle B_t^2\rangle}{\langle B_0^2\rangle}\right]^{-1/2}$$

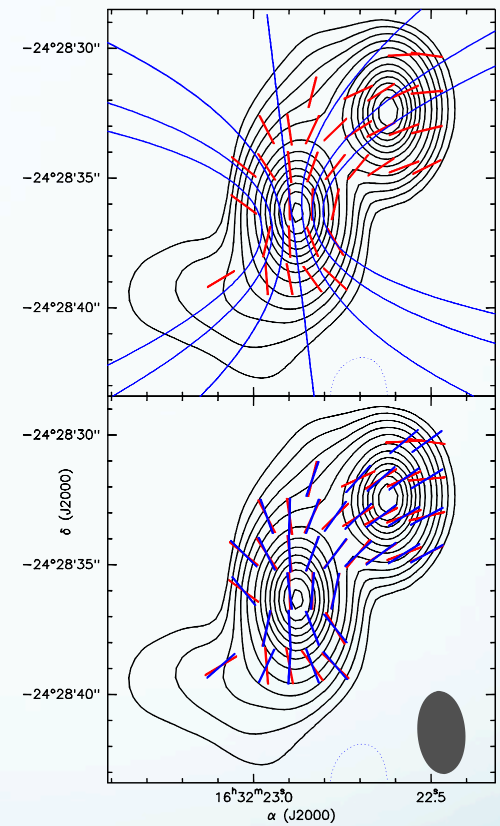

Rao et al. 2001

DR21 Filament in the Cygnus X Complex

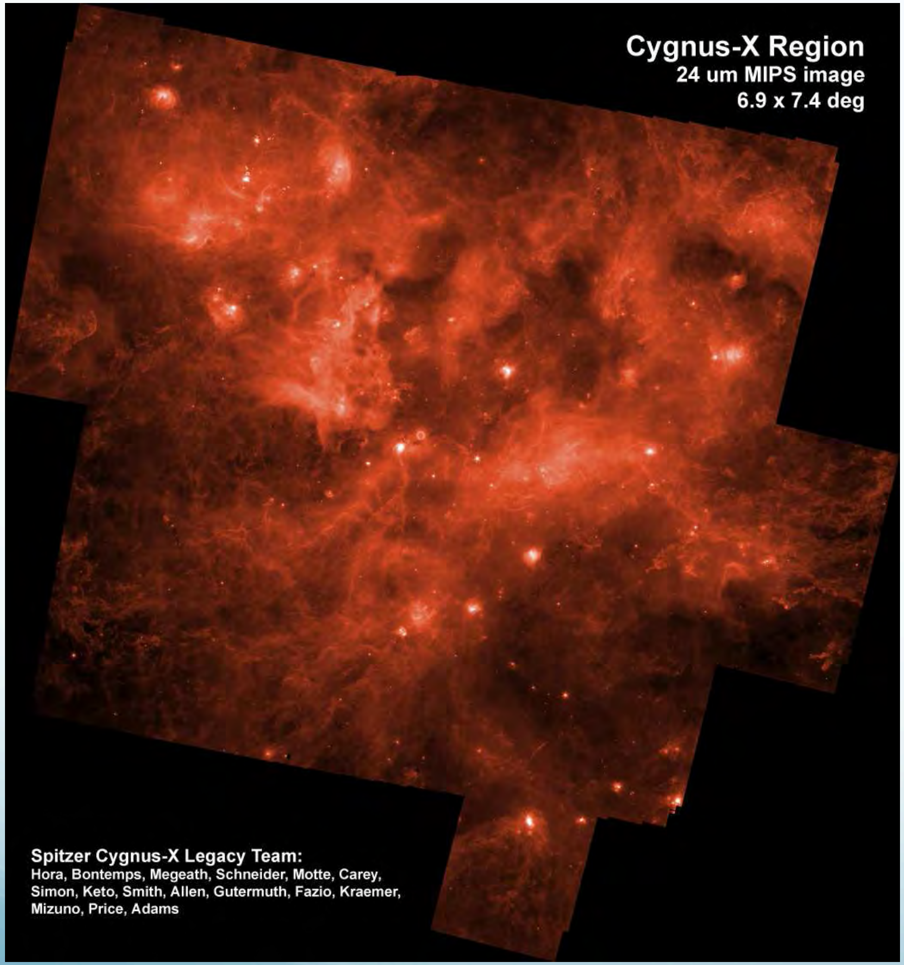

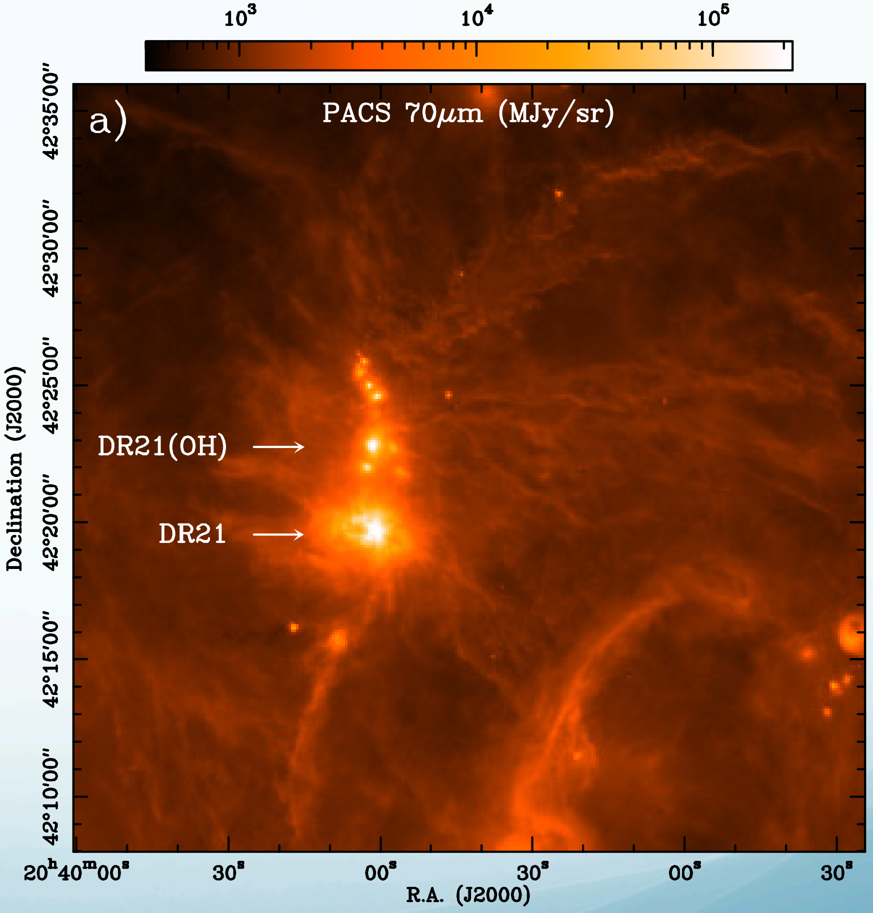

Hennemann et al. 2012

DR21 Filament

10 pc scale

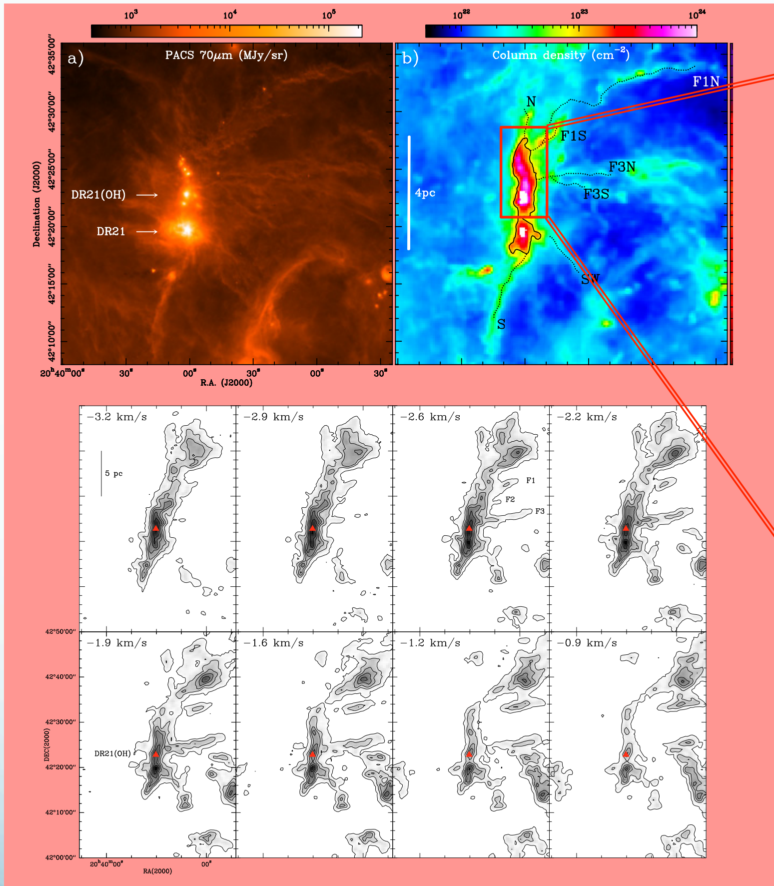

Motte et al. 2007;
Schneider et al, 2010;
Hennemann et al. 2012

1 pc scale

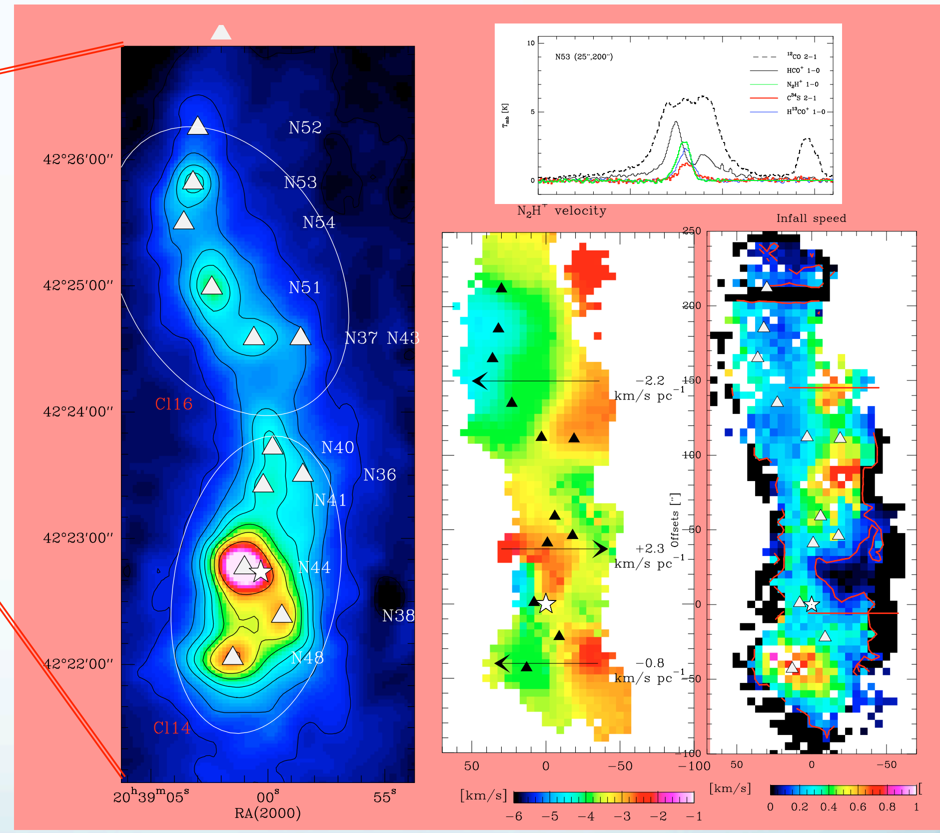

Mass: 15210 $M_\odot$
N_H: 4.2 x 10^{23} cm^{-2}
n_H: 10^5 cm^{-3}

Length: 4.3 pc
Width: 0.24 pc

Massive Cores in the DR21 Filament

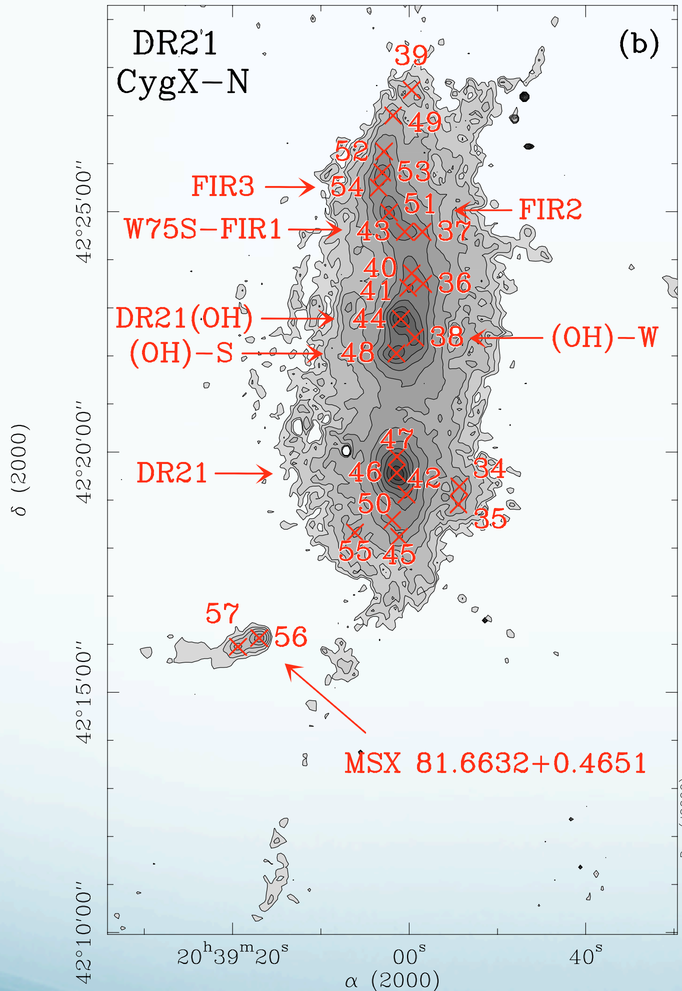

Motte et al. 2007

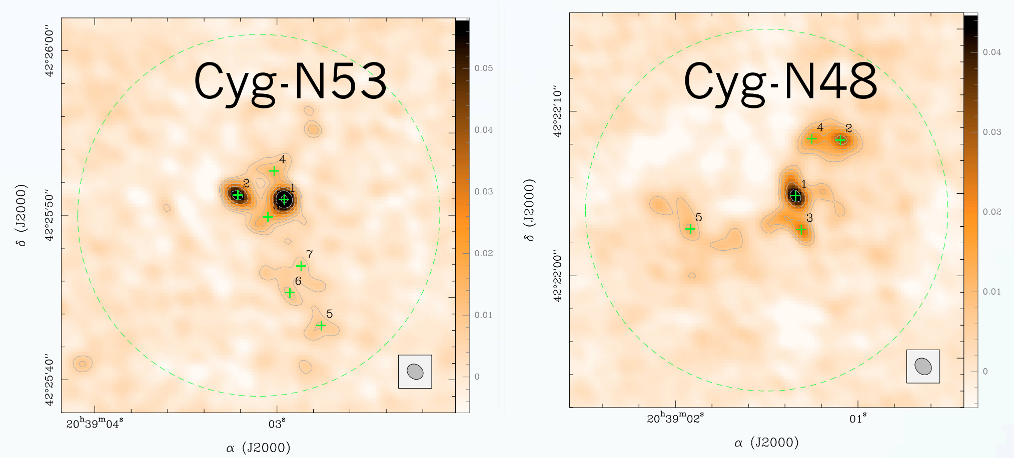

Bontemps et al. 2013

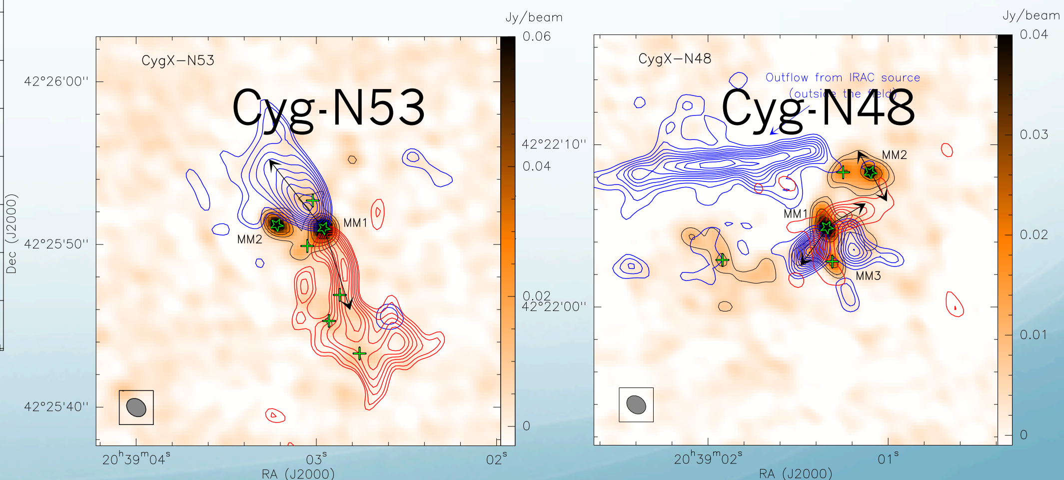

Duarte-Cabral et al. 2013

Measurements of Magnetic Fields

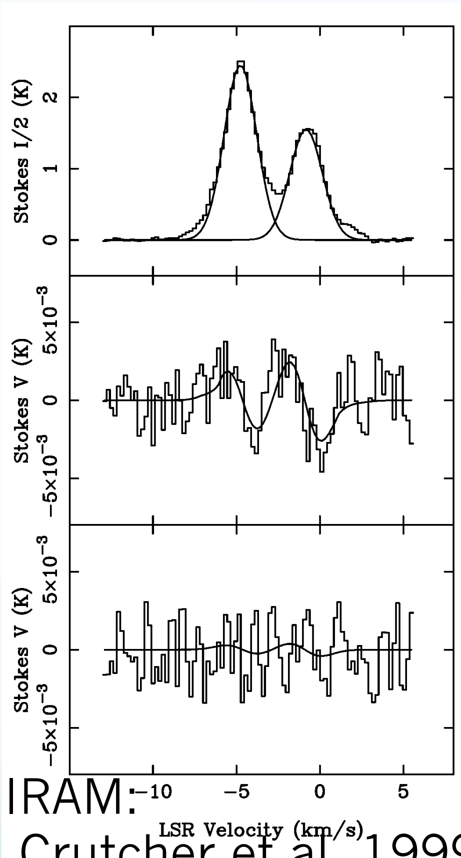

IRAM: Crutcher et al. 1999

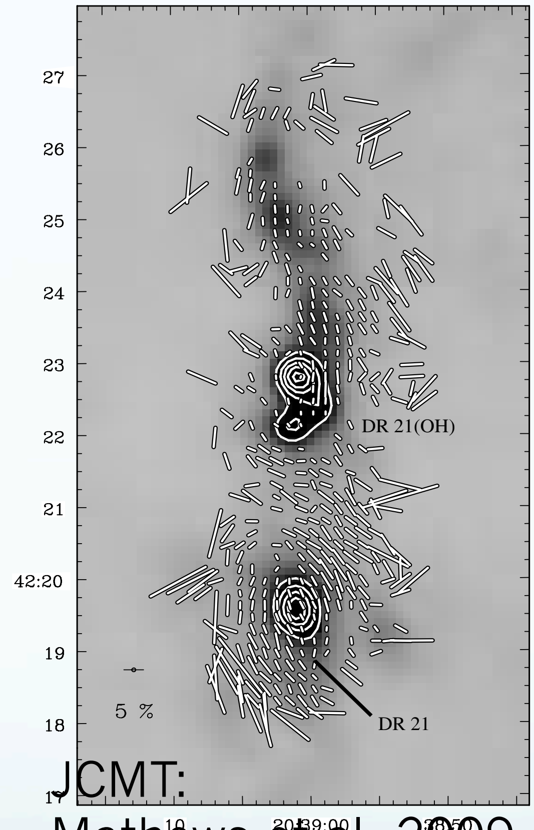

JCMT: Mathews et al. 2009

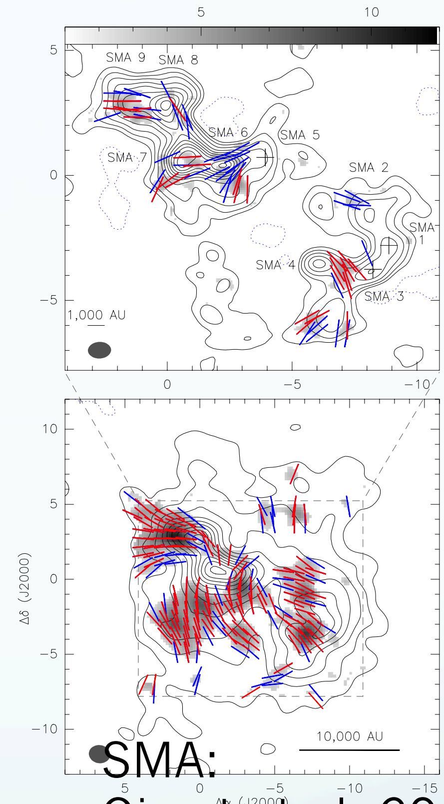

SMA: Girart et al. 2013

- DR21 Filament
  - Blos: 0.7 mG
  - Bpos: 0.62 mG

- DR21(OH)
  - Blos: 0.4 mG
  - Bpos: 2.1 mG (Girart et al. 2013); 1.2 mG (Houde et al. 2016)

SMA Polarization Observations

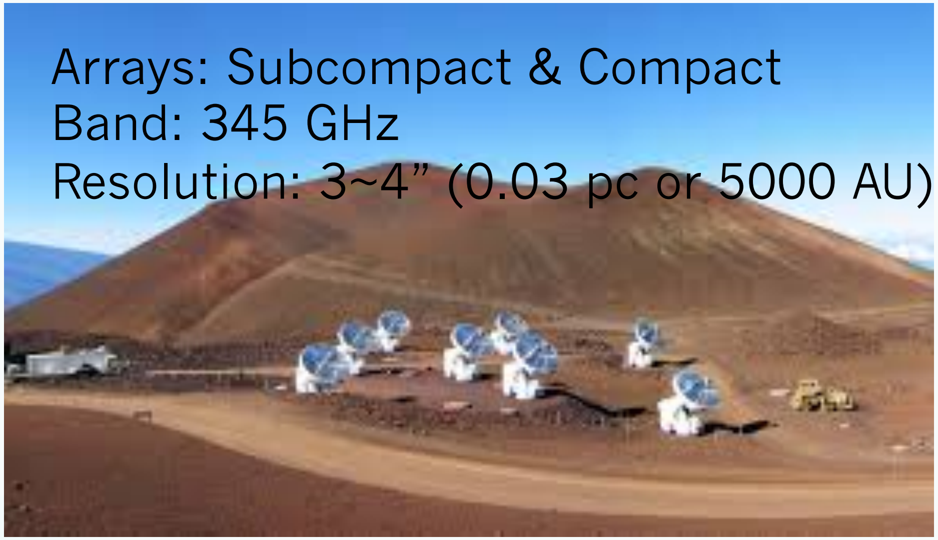

Arrays: Subcompact & Compact
Band: 345 GHz
Resolution: 3~4" (0.03 pc or 5000 AU)

Source	RA	Dec	Other Name
Cyg-N53	20:39:2.96	42:25:51	DR21(OH)-N
Cyg-N51	20:39:2.4	42:24:59	W75N-FIR2
Cyg-N43	20:39:0.6	42:24:35	W75S-FIR1
Cyg-N44	20:39:0.7	42:22:46.7	DR21(OH)
Cyg-N38	20:38:59.1	42:22:26	DR21(OH)-W
Cyg-N48	20:39:1.3	42:22:4.9	DR21(OH)-S

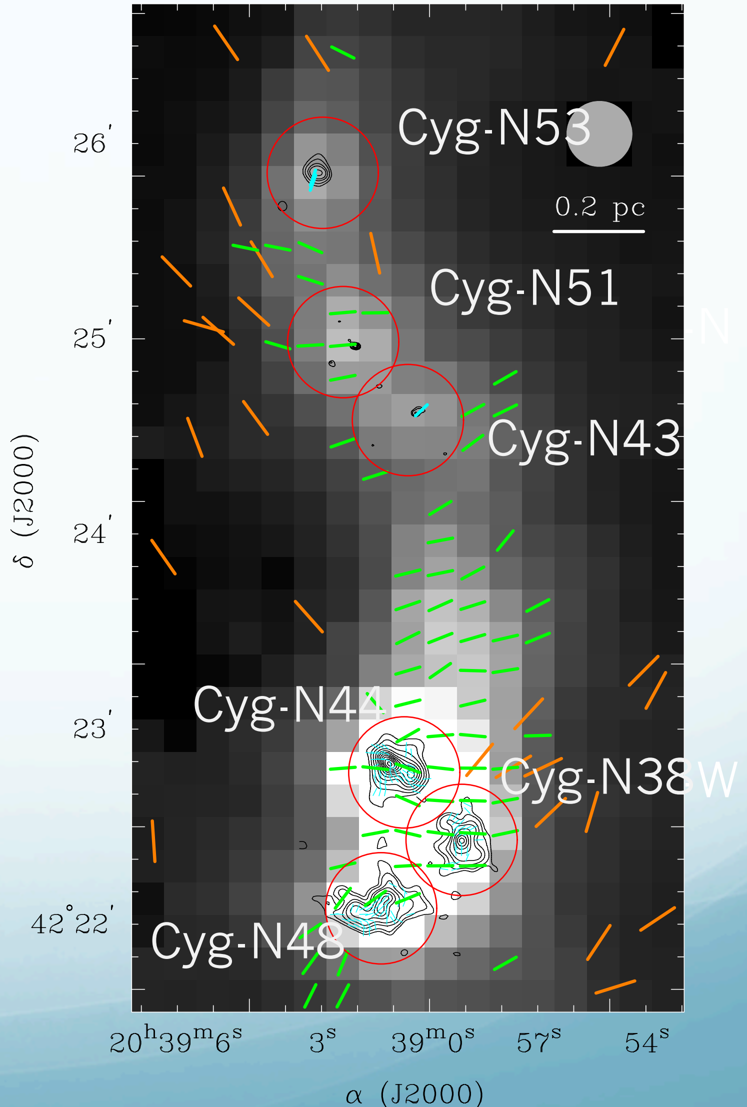

Results

- All segments show B-field direction
- Red & Yellow: JCMT
- Blue: SMA

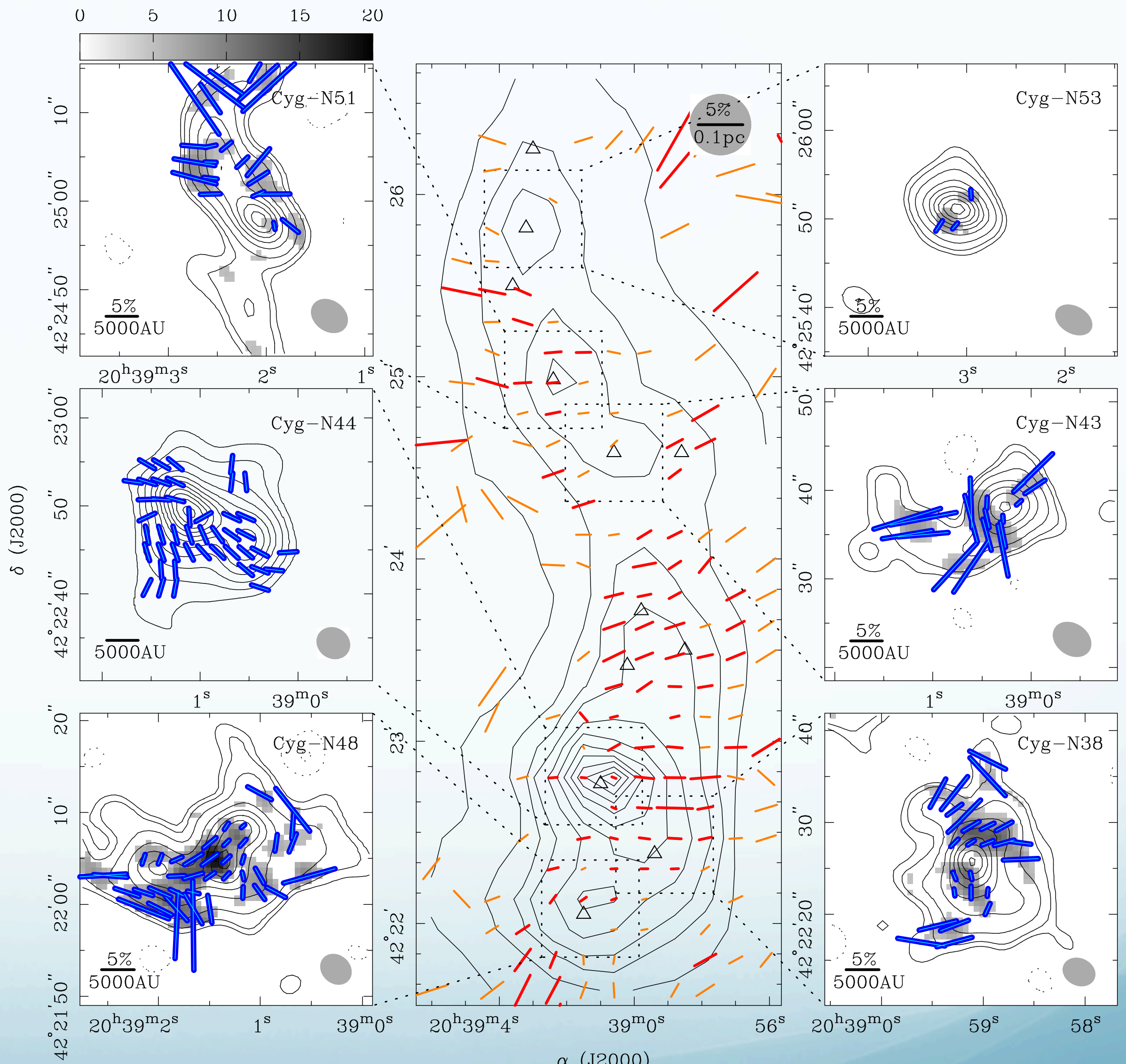

Combined JCMT and SMA 880 μm continuum maps

- Use FEATHER in casa and LINMOS in miriad
- Combine Stokes I maps, NOT combine Stokes Q and U maps
- Perform *dendrograms* to estimate core properties (Mass, Size, Density, P.A.)

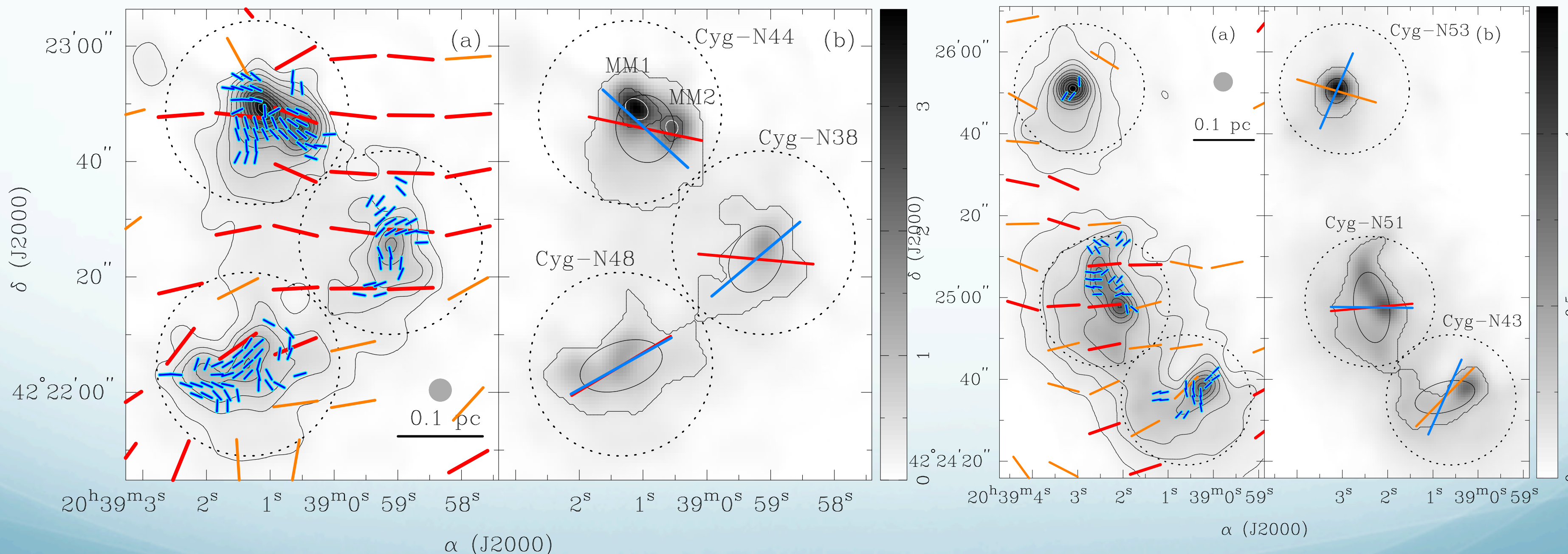

Analysis

Correlations between Core P.A. (0.1 pc core), JCMT pol (0.1 pc B-field), SMA pol (0.03 pc B-field)

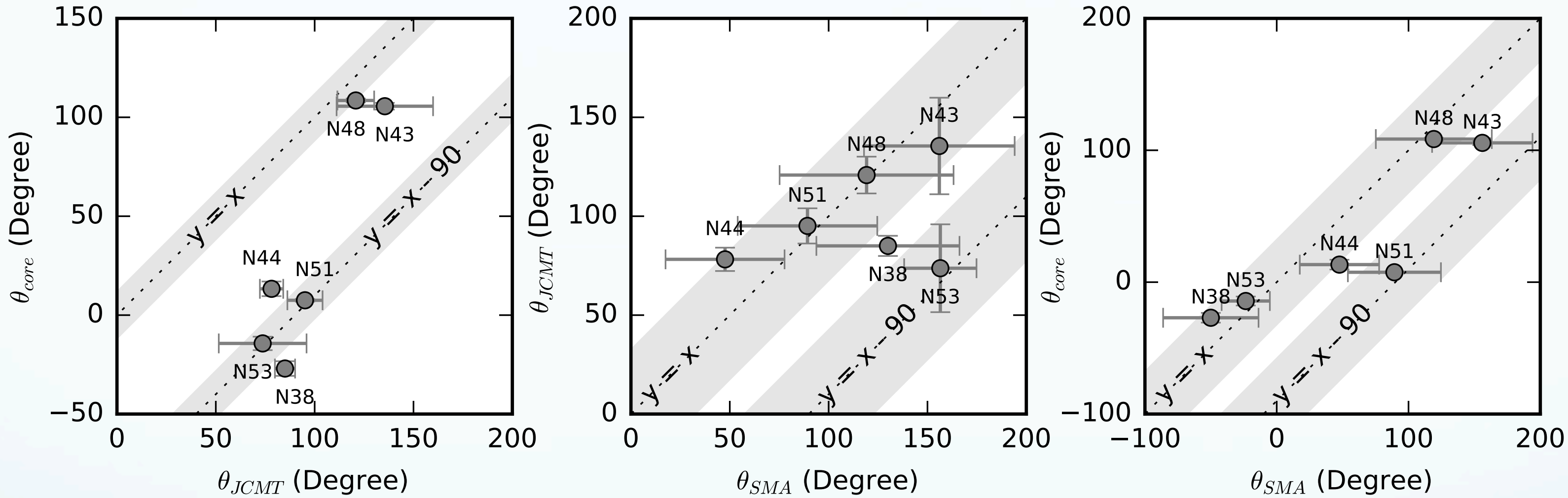

- Strong either-parallel-or-perpendicular alignment between 0.1 pc core and 0.1 pc B-field, weak correlation between 0.1 pc core and 0.03 pc B-field
  - small-scale B-field is less significant than large-scale B-field in core formation

- Does the either-parallel-or-perpendicular alignment break at scales below 0.1 pc?

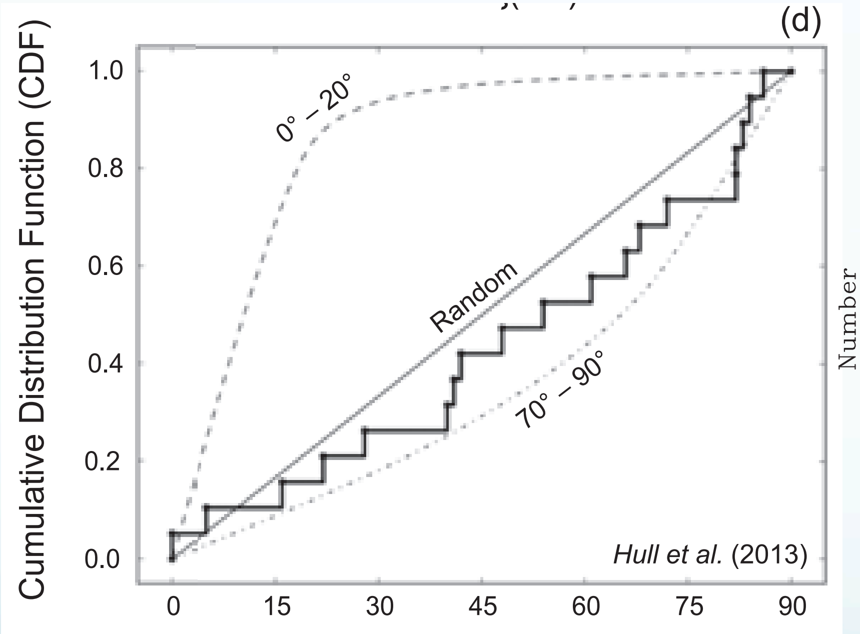

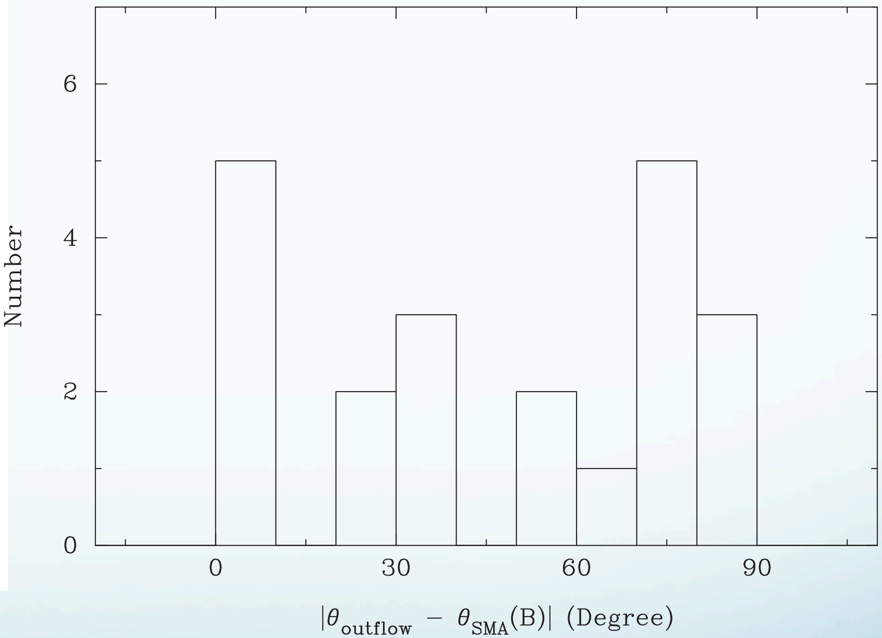

Low-mass protostars
Outflow and B-field alignment
Hull et al. 2013

High-mass protostars
Outflow and B-field alignment
Zhang et al. 2014

- Angular dispersion functions of the massive cores
  - The functions close to random field
    - strong turbulent component in the B-field
  - B_{pos} (mG)
    - Cyg-N38: 0.56 ± 0.19
    - Cyg-N43: 0.42 ± 0.41
    - Cyg-N44: 1.71 ± 0.55
    - Cyg-N48: 0.48 ± 0.10
    - Cyg-N51: 0.46 ± 0.08
    - DR21 filament: ~ 0.62 (Girart et al. 2013)

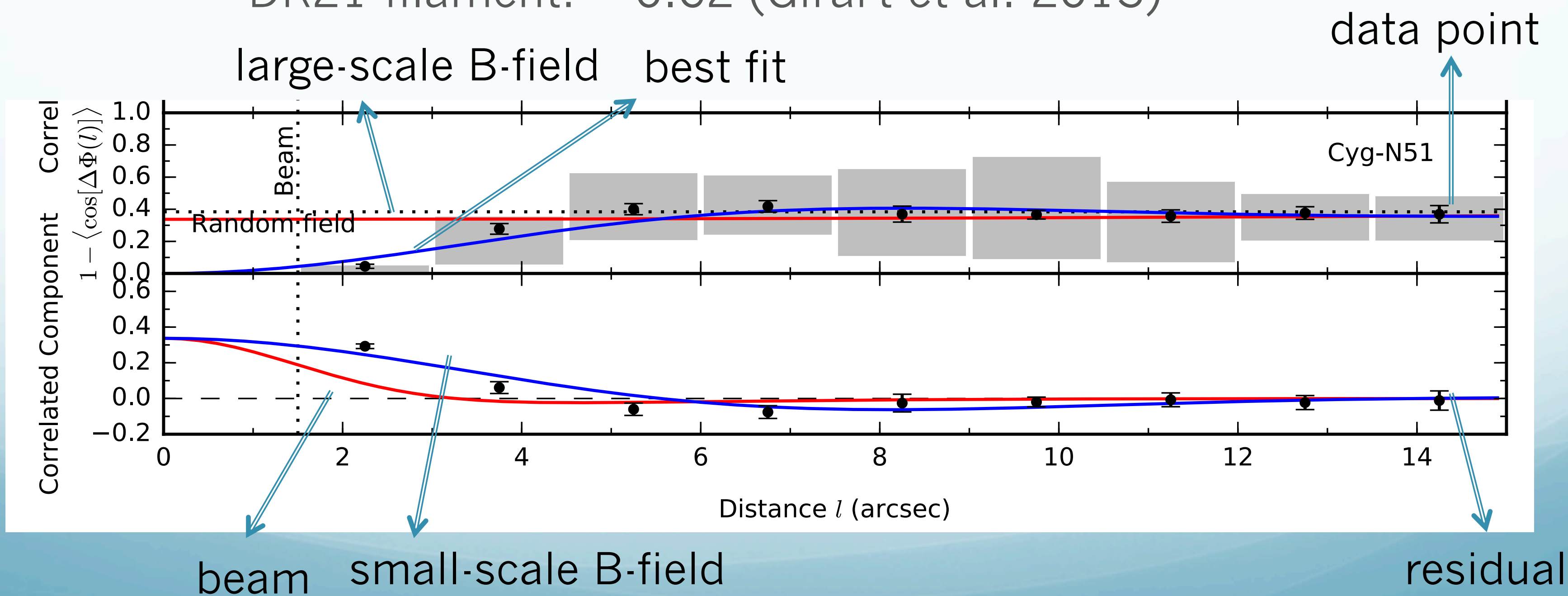

- Total B-field strength v.s. n_{H2}
  - Cyg-N44 and DR21 filament: combine B_{los} from Zeeman observations and B_{pos} in our work
  - Other sources: assume $B_{total} = \sqrt{3} B_{los}$, uncertainty about 50%
- Slope = 0.54 ± 0.30

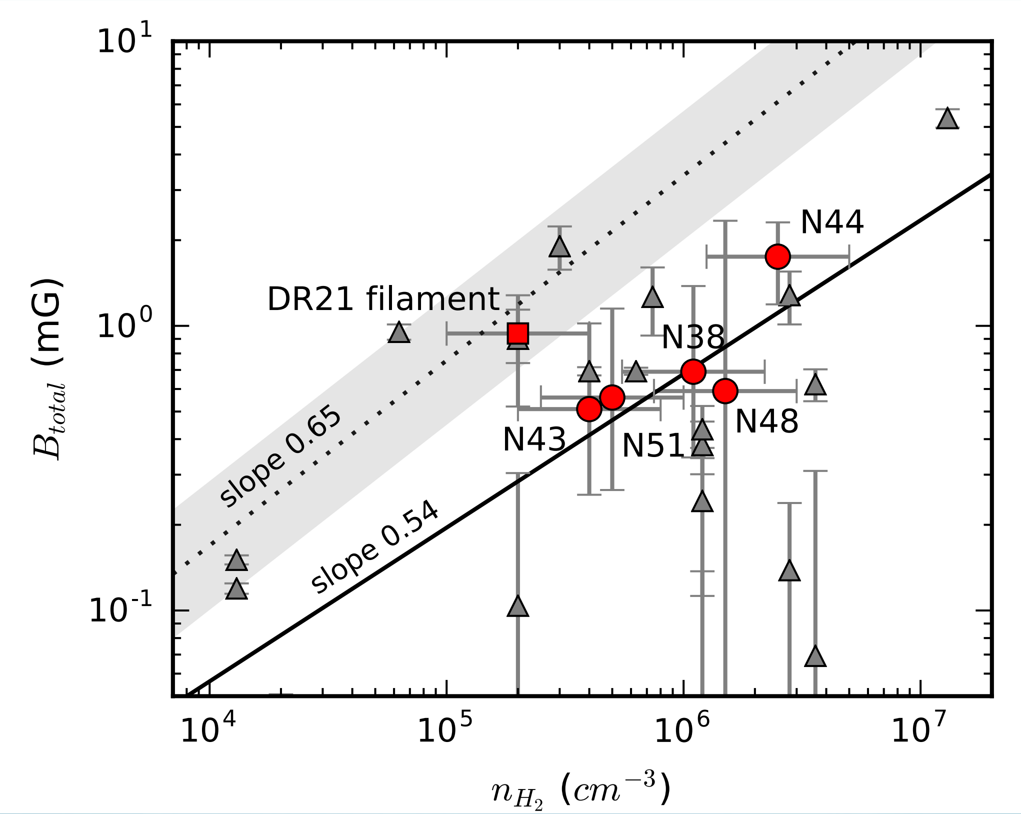

- $B \sim n_H^k$
  - $k = 2/3$ for weak magnetic field models (flux conservation)
  - $k = 0.4$-0.5 for strong magnetic field models (ambipolar diffusion)
- $k = 0.65 \pm 0.05$ (Crutcher et al. 2010)
- $k = 0.41 \pm 0.04$ in NGC 6334 (Li et al. 2015)

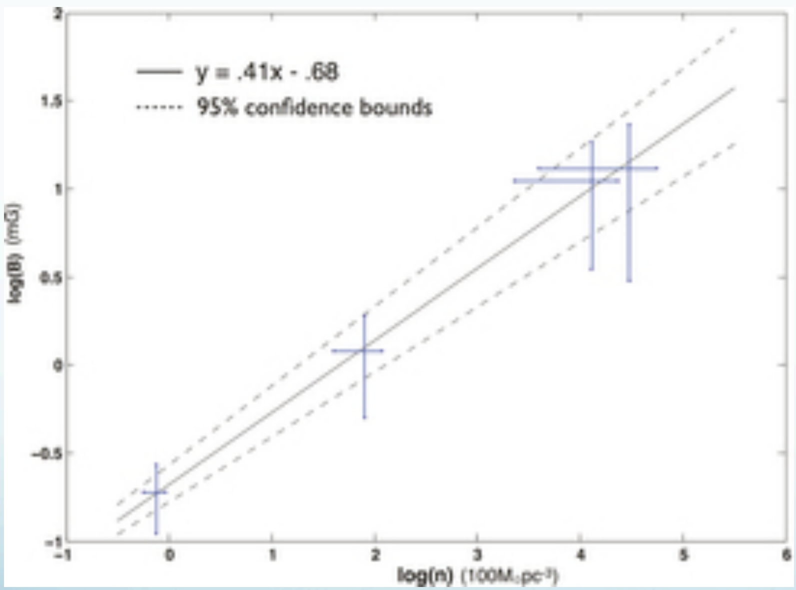

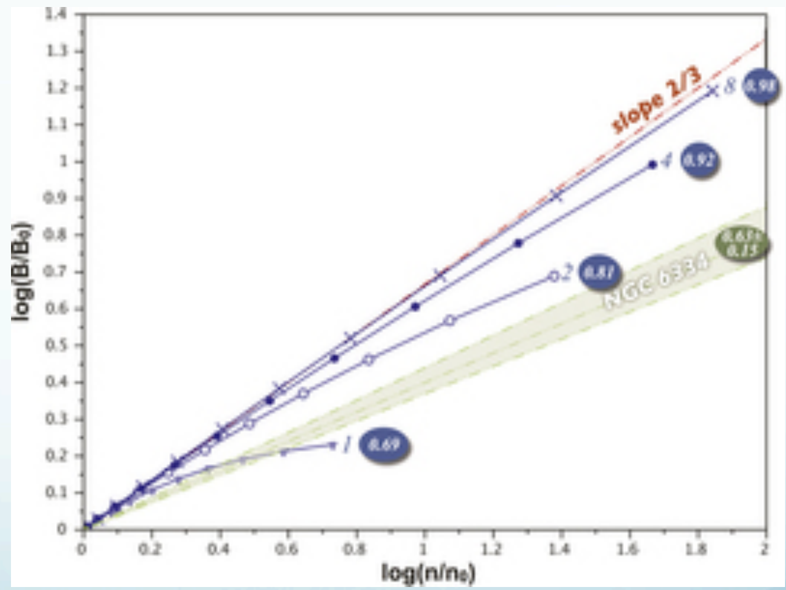

Li et al. 2015

- Parameters for evaluating the effects of turbulence, magnetic fields, and self-gravity
  - sonic Mach number (m_s), Alfven Mach number (m_A), ratio of thermal to magnetic pressure (β)
    - cores: $m_s > m_A > 1 > \beta$, turbulence dominant
    - filament: $m_s > 1 > m_A > \beta$, B-field dominant
  - Mass-to-flux ratio (M/Φ_B) ≥ 1, B-field cannot support self-gravity
  - Virial parameters
    - cores: *T*(turbulence) > *M* (B-field) > *W* (gravity)
    - filament: *W* > *M* > *T*
    - Expanding core in contracting filament?
      - Not consider surface terms, e.x. cloud colliding
      - refill turbulence from internal origin, e.x. outflows

Source	c_s (km s^{-1})	σ_v (km s^{-1})	V_A (km s^{-1})	m_s	m_A	β	M/Φ_B $(1/2\pi\sqrt{G})$	$\lvert\frac{\mathcal{T}}{\mathcal{W}}\rvert$	$\lvert\frac{\mathcal{M}}{\mathcal{W}}\rvert$	$\lvert\frac{2\mathcal{T}+\mathcal{M}}{\mathcal{W}}\rvert$
Cyg-N38	0.34	1.5	0.9	7.5	2.7	0.27	2.4	1.4	0.19	3.0
Cyg-N43	0.34	1.6	1.2	8.0	2.4	0.18	1.0	5.7	0.99	12.4
Cyg-N44	0.42	2.2	1.6	9.0	2.4	0.14	2.3	1.2	0.20	2.6
Cyg-N48	0.34	1.2	0.7	6.0	3.0	0.50	4.3	0.6	0.06	1.3
Cyg-N51	0.34	1.6	1.1	8.0	2.4	0.18	1.6	2.5	0.42	5.4
DR21 Filament	0.30[a]	0.8	3.0[b]	4.6	0.5	0.02	3.4[c]	0.04	0.28	0.36

Conclusions

- Highly turbulent cores
  - scattered SMA polarization segments
  - the analysis of angular dispersion function is similar to random B-fields
  - weak correlation between with the core and B-field orientation
  - B_{pos} = 0.4—1.7 mG
  - $B \sim n_H^{0.54}$
  - $m_s > m_A > 1 > \beta$, turbulence dominant
  - T(turbulence) > M (B-field) > W (gravity)

- Highly magnetized filament
  - ordered JCMT polarization segments, B-field perpendicular to the filament
  - either-parallel-or-perpendicular alignment between core and B-field
  - $m_s > 1 > m_A > \beta$, B-field dominant
  - W (gravity) > M (B-field) T(turbulence)

SMA Polarization Mosaic Project

PI: Tao-Chung Ching

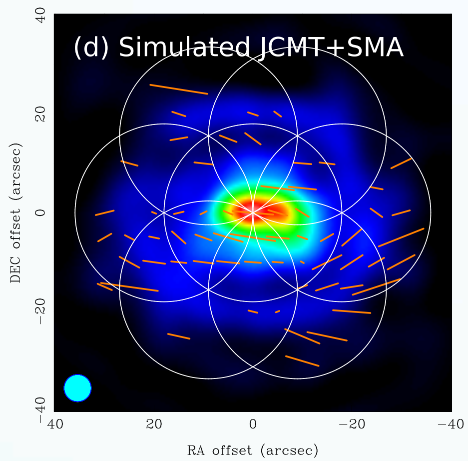

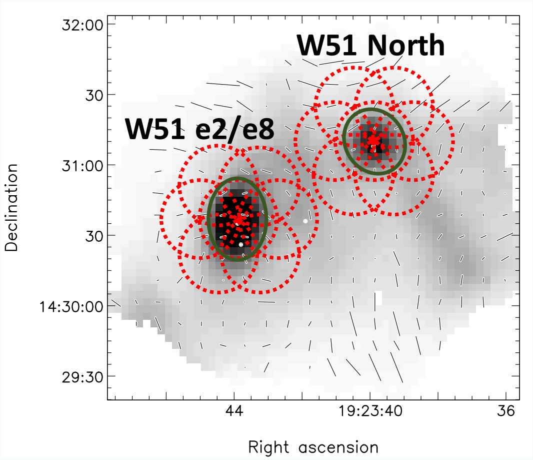

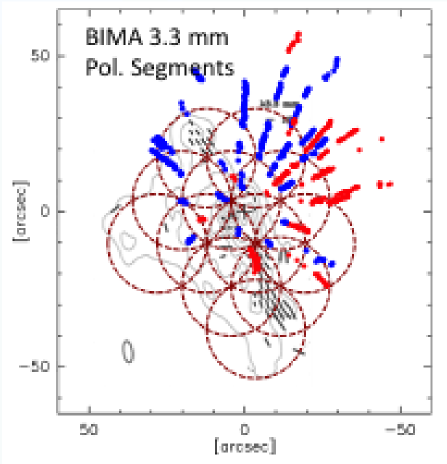

- NTHU: Shih-Ping Lai, Eswaraiah Chakali, Huei-Ru Chen, Jia-Wei Wang
- ASIAA: Ya-Wen Tang, Hsi-Wei Yen, Patrick M. Koch, Ramprasad Rao, Naomi Hirano, Shang Hsien, Ruben Krasnopolsky, Chin-Fei Lee, Wing-Kit Lee, Sheng-Yuan Liu, Shigehisa Takakuwa, Liang-Yao Wang
- CfA: Qizhou Zhang, Ken Young, Glen Petitpas, Ryan Howie
- Institue de Ciencies de l'Espai: Josep M. Girart

- Stokes I mosaic observations
- Single-point polarization observations

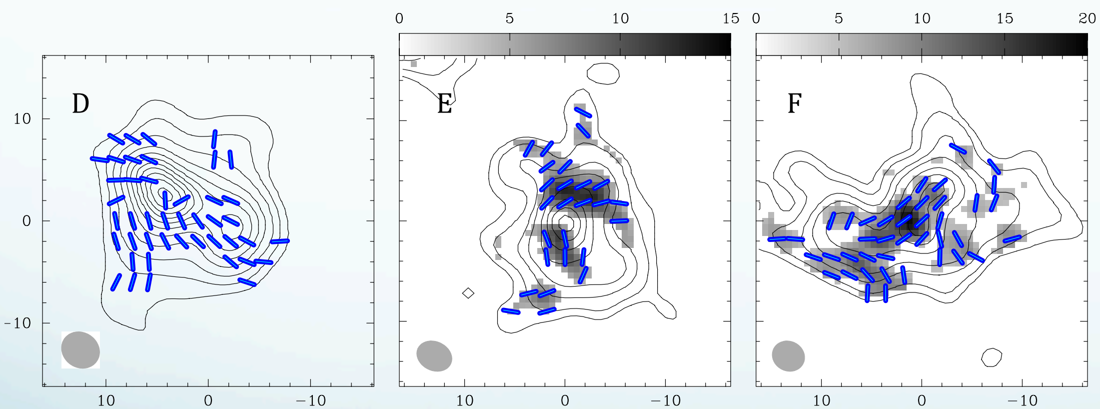

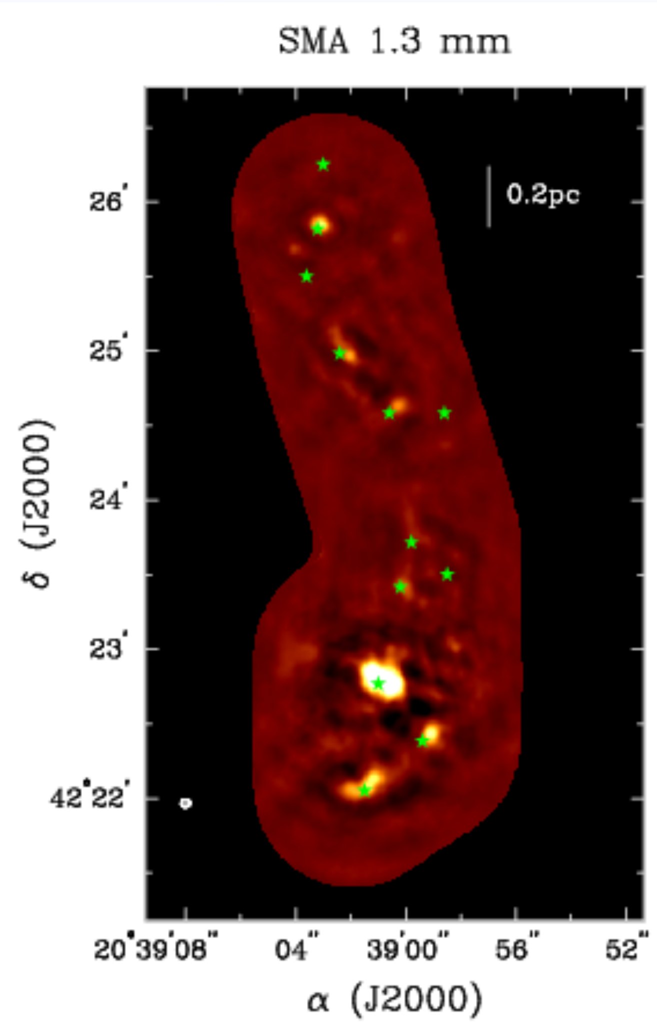

- Measurements of SMA off-axis instrumental polarization

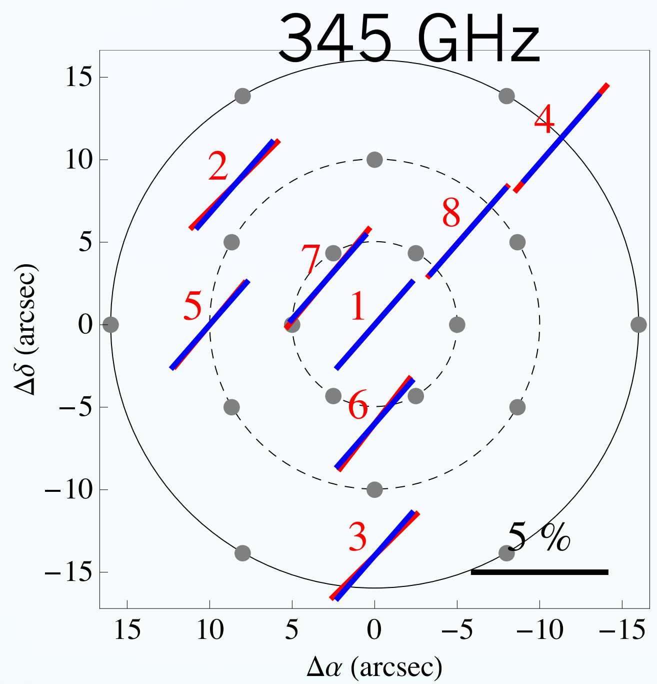

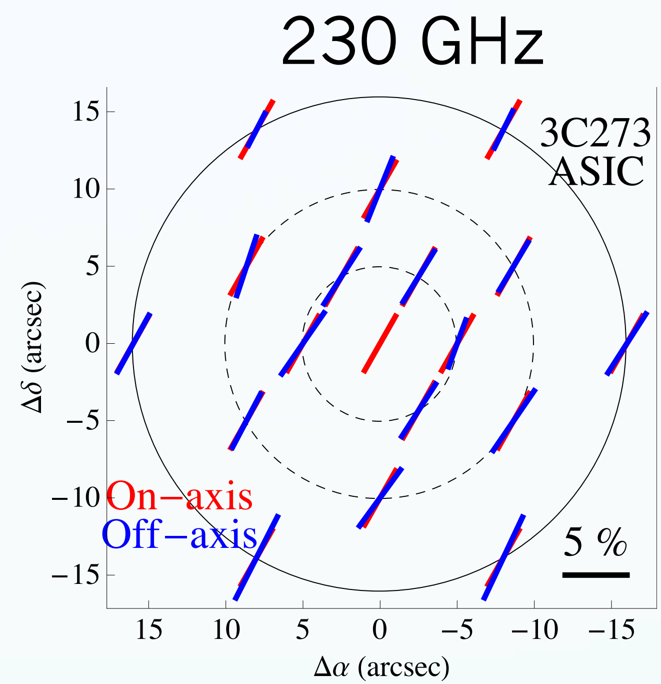

- $\Delta P = 0.3 \pm 0.1\%$
- $\Delta P.A. < 5^0$

Table 1: SMA off-axis polarization measurements of 3C279

Position	Stokes Values (Jy/beam)			Pol (%)	PA (°)	Residual Polarization	
	I	Q	U			ΔPol (%)	ΔPA (°)
1	10.27	-0.059	-0.434	4.26 ± 0.08	138.9 ± 0.5	–	–
2	8.18	0.001	-0.373	4.56 ± 0.10	135.0 ± 0.6	0.30 ± 0.13	-3.9 ± 0.8
3	6.20	0.003	-0.277	4.47 ± 0.13	134.7 ± 0.8	0.21 ± 0.15	-4.2 ± 1.0
4	4.38	-0.033	-0.226	5.20 ± 0.18	139.2 ± 1.0	0.94 ± 0.20	0.3 ± 1.1
5	8.37	-0.062	-0.337	4.09 ± 0.10	140.2 ± 0.7	-0.17 ± 0.13	1.3 ± 0.8
6	9.14	-0.100	-0.380	4.30 ± 0.09	142.4 ± 0.6	0.04 ± 0.12	3.5 ± 0.8
7	9.98	-0.086	-0.471	4.79 ± 0.08	140.1 ± 0.5	0.53 ± 0.11	1.2 ± 0.7
8	8.45	-0.050	-0.376	4.49 ± 0.09	138.8 ± 0.6	0.23 ± 0.12	-0.2 ± 0.8

- Multiple pointing polarization data of extended sources from SMA archive

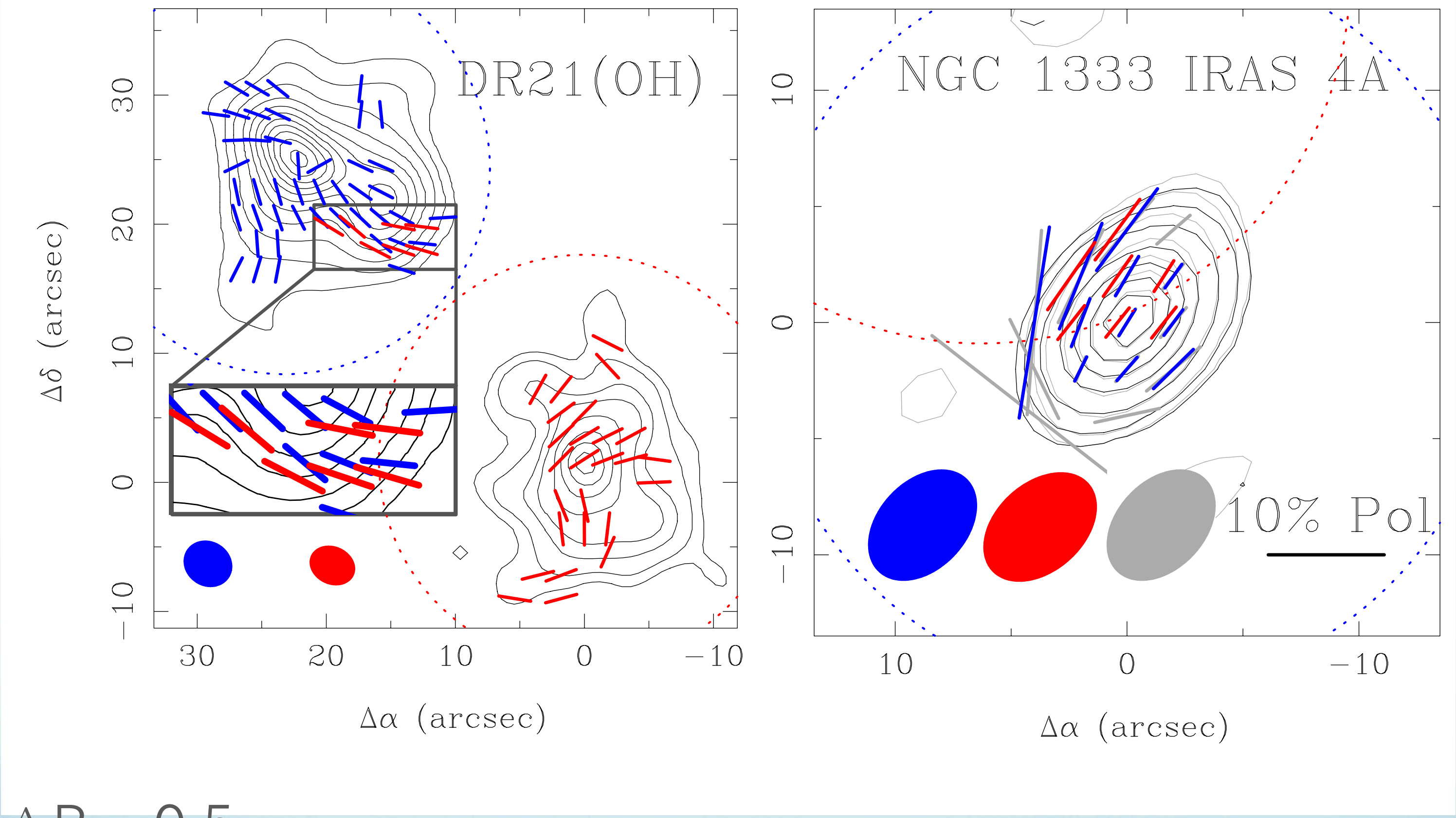

- ΔP ~ 0.5
- ΔP.A. = 6^0 at a distance of 30”, 9^0 at a distance of 40”

- Pilot observations
  - W51 e2/e8 & W51 north

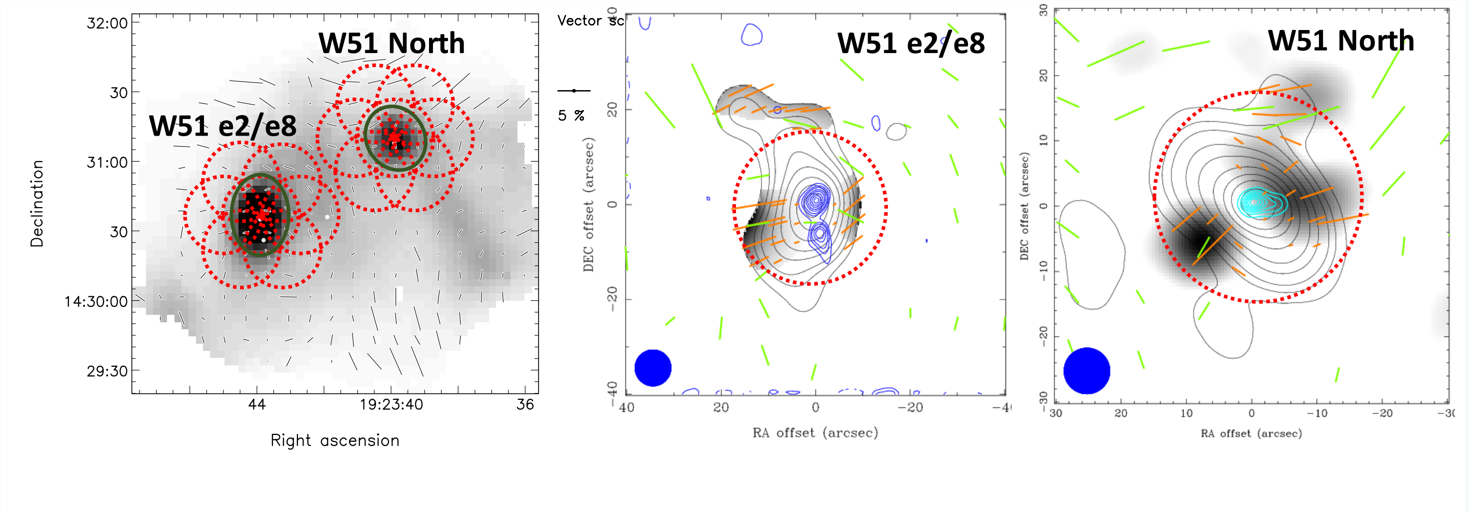

  - Orion BN/KL

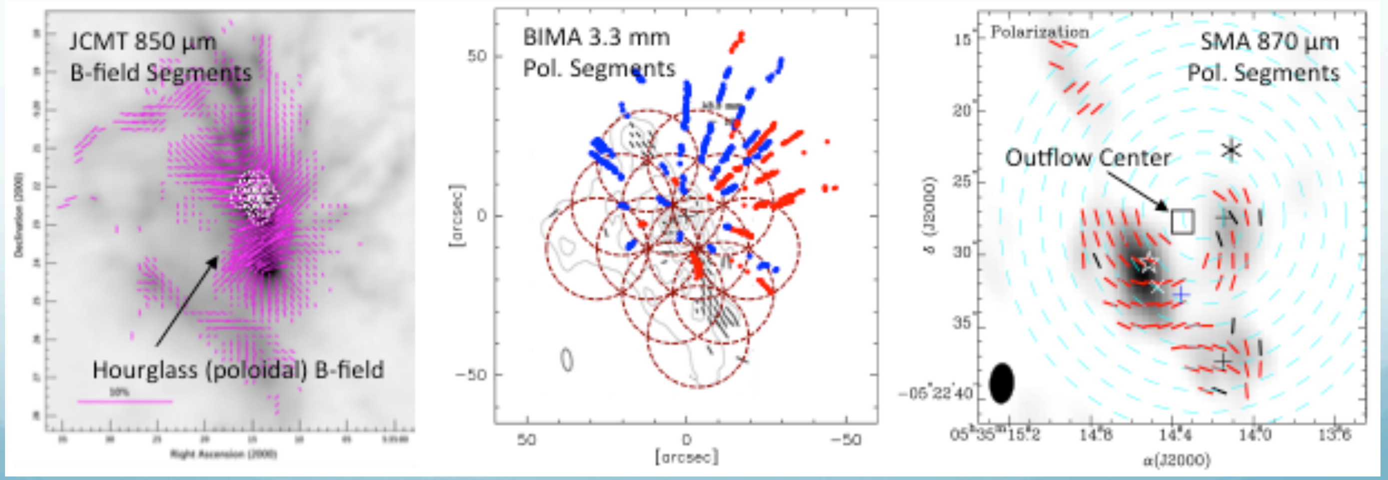

- Bistro legacy project (A magnetic field survey of the Gould Belt clouds), PI: Derek Ward-Thompson
- Members from Taiwan: Ya-Wen Tang, Patrick Koch, Vivien Chen, Shi-Ping Lai, Jia-Wei Wang, Sheng- Yuan Liu, Hsi-Wei Yen, Tao-Chung Ching

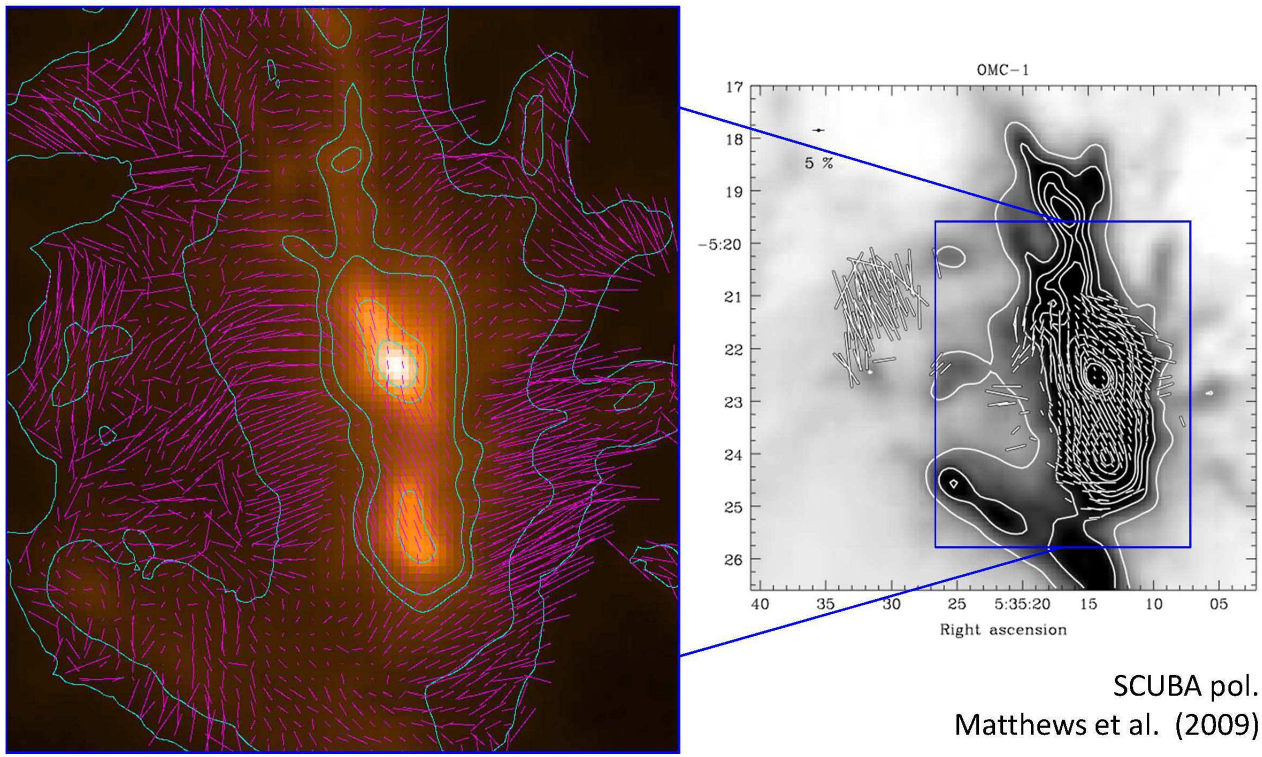

SCUBA pol.
Matthews et al. (2009)

OMC-1
Commissioning Data

JCMT + SMA polarization mosaic map

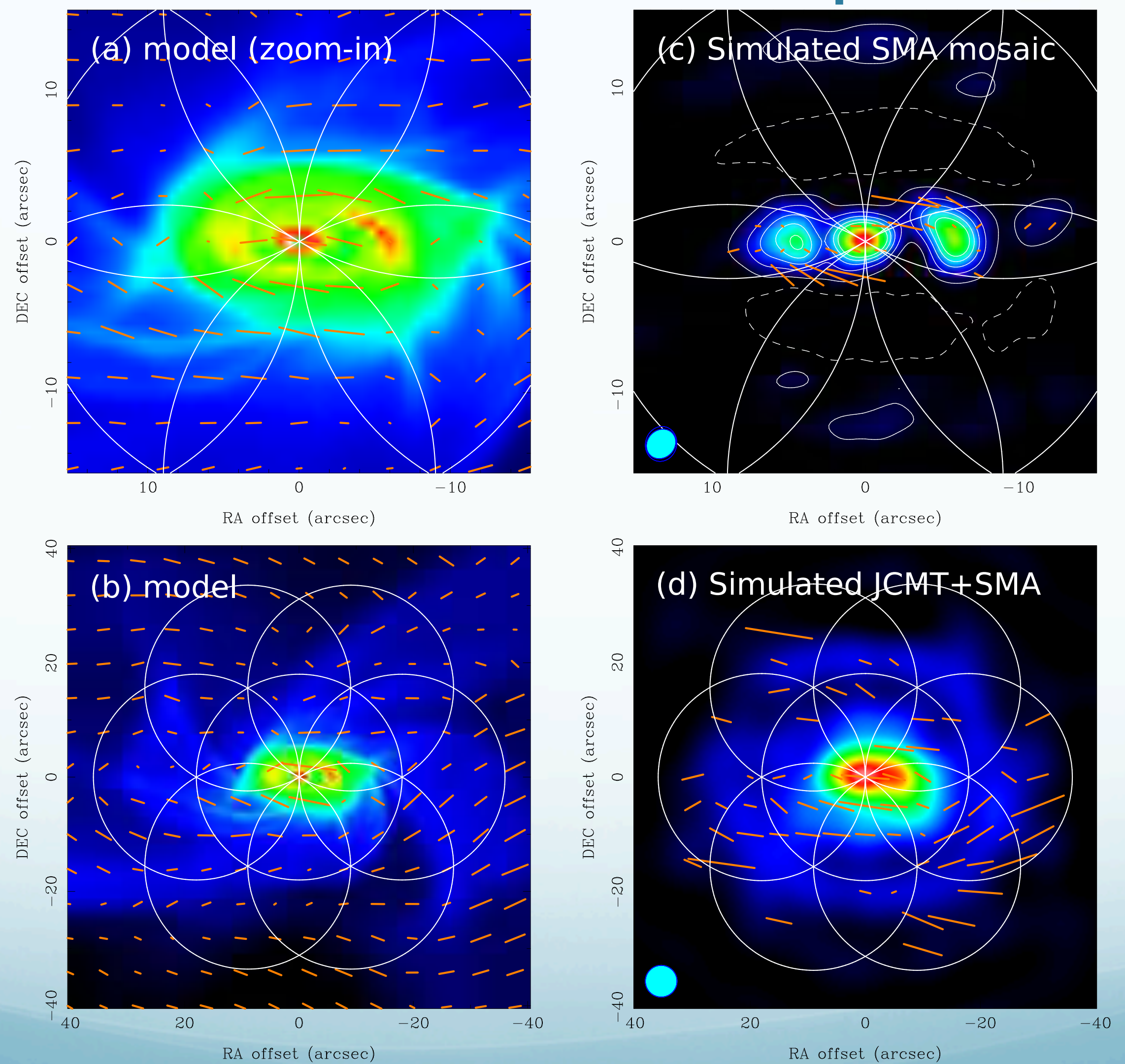

Thank you for your attention